SMALL SCALE DISCHARGE STUDIES

J.H. Jacob and J.A. Mangano
Avco Everett Research Laboratory, Inc.
2385 Revere Beach Parkway
Everett MA 02149

Semi–Annual Report for Period 1 September 1975 to 29 February 1976

Sponsored by
DEFENSE ADVANCED RESEARCH PROJECTS AGENCY
DARPA Order No. 1806

Monitored by
OFFICE OF NAVAL RESEARCH
DEPARTMENT OF NAVY
Arlington VA 22217

DISCLAIMER NOTICE

THIS DOCUMENT IS THE BEST QUALITY AVAILABLE.

COPY FURNISHED CONTAINED A SIGNIFICANT NUMBER OF PAGES WHICH DO NOT REPRODUCE LEGIBLY.

FOREWORD

DARPA Order No.: 1806

Program Code No: 5E20

Name of Contractor: Avco Everett Research Laboratory, Inc.

Effective Date of Contract: 15 August 1974

Contract Expiration Date: 14 August 1976

Amount of Contract: $429,588

Contract No.: N00014-75-C-0062

Principal Investigator and Phone No.: J.H. Jacob
(617) 389-3000, Ext. 329

Scientific Officer: Director, Physics Program Physical Sciences Div.
Office of Naval Research
Department of the Navy
800 North Quincy Street
Arlington, VA. 22217

Short Title of Work: Laser Discharge Studies

UNCLASSIFIED

SECURITY CLASSIFICATION OF THIS PAGE *(When Data Entered)*

REPORT DOCUMENTATION PAGE

READ INSTRUCTIONS BEFORE COMPLETING FORM

1. REPORT NUMBER

2. GOVT ACCESSION NO.

3. RECIPIENT'S CATALOG NUMBER

4. TITLE *(and Subtitle)*

Small Scale Discharge Studies •

5. TYPE OF REPORT & PERIOD COVERED

Semi-Annual Report •
1 Sept. 1975 to 29 Feb. 1976

6. PERFORMING ORG. REPORT NUMBER

7. AUTHOR(s)

J. H. Jacob and J. A. Mangano

8. CONTRACT OR GRANT NUMBER(s)

N00014-75-C-0625
DARPA Order-1806

9. PERFORMING ORGANIZATION NAME AND ADDRESS

Avco Everett Research Laboratory, Inc.
2385 Revere Beach Parkway

10. PROGRAM ELEMENT, PROJECT, TASK AREA & WORK UNIT NUMBERS

11. CONTROLLING OFFICE NAME AND ADDRESS

Defense Advanced Research Projects Agency
DARPA Order No. 1806

12. REPORT DATE

29 Feb 76

13. NUMBER OF PAGES

61

14. MONITORING AGENCY NAME & ADDRESS *(if different from Controlling Office)*

Office of Naval Research
Department of Navy
Arlington, VA 22217

15. SECURITY CLASS. *(of this report)*

Unclassified

15a. DECLASSIFICATION/DOWNGRADING SCHEDULE

16. DISTRIBUTION STATEMENT *(of this Report)*

Approved for Public Release; Distribution Unlimited

17. DISTRIBUTION STATEMENT *(of the abstract entered in Block 20, if different from Report)*

18. SUPPLEMENTARY NOTES

19. KEY WORDS *(Continue on reverse side if necessary and identify by block number)*

Visible/UV Lasers
High Pressure Discharges
Rare Gas Fluoride Lasers
KrF* Laser

20. ABSTRACT *(Continue on reverse side if necessary and identify by block number)*

In the report we describe the modelling of an e-beam controlled discharge operated in gas mixtures containing mainly argon with approximately 10% krypton and a few tenths of a percent fluoride. The discharge physics is dominated by electron impact ionization and excitation of the rare gas metastables. The ionization of the metastables impacts the discharge stability directly while their excitation strongly effects the efficiency of producing

DD FORM 1 JAN 73 1473 EDITION OF 1 NOV 65 IS OBSOLETE

S/N 0102-014-6601

UNCLASSIFIED

SECURITY CLASSIFICATION OF THIS PAGE *(When Data Entered)*

(20)

KrF^*. Two step ionization is dominant and we have developed a stability criterion for these discharges. Predictions of the model are compared with experimental results.

REPORT SUMMARY

In the period from September 1975 to February 1976, we have actively investigated the discharge physics of the rare gas fluoride lasers. KrF* prototypical of this class of lasers.

Shortly after lasing of KrF* was obtained in a discharge, the discharge physics was thoroughly researched. We determined that the discharge physics was dominated by electron impact of the rare gas metastables. The dominant ionization was two step ionization. Fortunately, the discharge can be stabilized if the attachment rate is twice the equilibrium ionization rate. This stability criteria was derived theoretically and verified experimentally. Details of the theory and experiment are discussed in the following sections. Under stable discharge conditions, we have obtained metastable production efficiencies of 70% with discharge enhancements (discharge power/e-beam power) of 3-4.

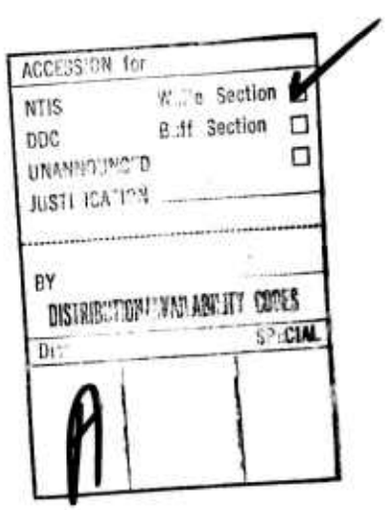

TABLE OF CONTENTS

LIST OF ILLUSTRATIONS

I. INTRODUCTION

ARPA/ONR sponsored laser programs at AERL have recently led to the discovery of several rare gas-monohalide laser systems.[1-4] This new class of laser offers the potential of both high overall electrical efficiency (≥10%) and high average laser power (≥100 kW/aperture). In particular, under the ARPA/ONR sponsored Laser Discharge Studies program for FY 75, e-beam controlled discharge pumping of the KrF* laser at 248.5 nm was achieved (See Appendix A).[5] Pulse energies of 60 mJ at efficiencies of 1.4% have been achieved to date. In a well-designed, scaled-up version of this laser, these results have been extrapolated to give from 10-20% overall electrical efficiency. Scaling studies show that with discharge pumping this laser can give up to 1 MW average power per aperture.

The experiments were performed with existing apparatus that has been built under previous ARPA/ONR programs. The cold cathode electron gun provides a 150 keV beam of electrons with currents up to 25 A/cm^2. This beam is fired into a 20 cm long discharge cavity having a cross-sectional area of 2 x 2 cm^2. The discharge energy that is deposited into the laser mix is stored in a 0.3 μF capacitor. The capacitor, which can be charged up to 30 kV, is switched across the anode and cathode about 40 ns after the e-beam is fired.

(1) J.J. Ewing and C.A. Brau, App. Phys. Lett. 27, 350 (1975).
(2) C.A. Brau and J.J. Ewing, App. Phys. Lett. 27, 435 (1975).
(3) J.J. Ewing and C.A. Brau, App. Phys. Lett. 27, 350 (1975).
(4) J.J. Ewing and C.A. Brau, App. Phys. Lett. 27, 557 (1975).
(5) J.A. Mangano and J.H. Jacob, App. Phys. Lett. 27, 495 (1975).

II. DISCHARGE MODELING

In this report a model for the KrF laser discharge is given. The key physical processes dominating the discharge have been identified and are included in this model. The predictions of this model quantitatively agree with our discharge and fluorescence data over a wide range of discharge operating conditions. For example, the temporal evolution of the discharge current, voltage and the KrF fluorescence predicted by the model agree to within $\pm$ 20% of those observed experimentally. In addition, the model predicts that the efficiency of producing KrF* by discharge pumping can be as much as 50% higher than for direct e-beam pumping. (By e-beam pumping the efficiency of producing KrF* is predicted to be 22%).[6] The e-beam controlled discharge experiments which we report here also substantiate this prediction.

The physics of rare gas/halogen discharges is dominated by the excited species when the fractional population of the rare gas metastables exceeds 10^{-9}.[7, 8] For example, an important process in KrF laser discharges ($Kr^*/(Kr + Ar) \simeq 10^{-5}$) is the excitation of low lying metastables to higher lying states.[9] This process can strongly influence the secondary electron energy distribution and therefore the efficiency of producing the

(6) J.J. Ewing and C.A. Brau, unpublished.

(7) At fractional metastable populations of 10^{-9}, metastable ionization begins to dominate. The metastable production efficiency however is not affected until the fractional population reaches 10^{-5}.

(8) The possibility of the excited species having a strong effect on the discharge physics was brought to our attention by P.W. Hoff.

(9) In our code we have assumed that excitation of Kr^* to higher lying levels will result in an electron energy loss of 1.6 eV. This assumption is valid if the higher lying levels are rapidly quenched (by three-body processes) back to Kr^*.

metastables (which react with F_2 to form KrF^* -- the upper laser level). The dominant ionization mechanism in KrF laser discharges is ionization of the krypton and argon metastables, i.e., two-step ionization. For this discharge, metastable ionization rates of $1\text{-}5 \times 10^7$ sec^{-1} are typical so that this process strongly influences discharge stability. Fortunately this ionization can be balanced under certain conditions by fluorine attachment so that stable discharges are possible. These important excited state processes will be described in more detail in subsequent paragraphs. In particular, quantitative criteria will be developed for making rare gas metastables efficiently and for maintaining discharge stability. In addition it will be shown that efficient metastable production under stable discharge operating conditions can be achieved at large discharge enhancements (ratio of discharge power input to e-beam power input).

A. METASTABLE PRODUCTION EFFICIENCY

In our model the discharge is assumed to heat the secondary electrons produced by the e-beam until they have sufficient energy to make argon and krypton metastables. The krypton metastables are formed either by direct electron impact or by collisional transfer from argon metastables. It is then assumed that KrF^* is created by the following reactions:

$$Kr^* + F_2 \rightarrow KrF^* + F$$

or

$$Ar^* + F_2 \rightarrow ArF^* + F$$

followed by

$$ArF^* + Kr \rightarrow KrF^* + Ar$$

Since KrF is very weakly bound or unbound in the ground state,[10] KrF^* decays into krypton and fluorine after emitting a photon.

The discharge physics is, as we have stated previously, strongly affected by electron impact excitation and ionization of the rare gas metastables. To model these effects we have treated the krypton metastable as rubidium and the argon metastable as potassium. This analogy has been used successfully in predicting the emission spectra of the excited rare gas monohalides and is justified physically by the atomic similarity between rare gas metastables and the alkalis.[10] Some of the electron impact cross-sections used in our model are shown in Figure 1. The cross-section for excitation from the 5s configuration to the 5p configuration in Rb[11] (Kr^*) has a peak value of 75 $Å^2$ at 8 eV. Also shown are the ionization cross-section of Rb[12] and the excitation[13] and ionization[14] cross-sections of Ar. From Figure 1 it is clear that the peak value of the metastable excitation cross-section is 30 times the peak value of the argon excitation cross-section. More important, however, is that most of the electrons can excite the 5s to 5p transitions which have a threshold of 1.6 eV whereas only the high energy tail of the electron energy distribution can produce metastables from the ground state.

---

(10) C.A. Brau and J.J. Ewing, J. Chem. Phys. 63, 4640 (1975).

(11) H. Hyman, private communication.

(12) R.H. McFarland and J.D. Kinney, Phys. Rev. 137, 1058 (1965).

(13) The shape of the total excitation cross-section was obtained from H.S.W. Massey and E.H.S. Bishop, Electronic and Ionic Impact Phenomena, Vol. I, p. 259. To obtain the amplitude of the cross-section we used the Boltzmann code. The amplitude shown in Figure 1 gave the best fit to the first Townsend coefficient that was measured by D.E. Golden and L.H. Fisher, Phys. Rev. 123, 1079 (1961).

(14) D. Rapp and P. Englander-Golden, J. Chem. Phys. 43, 1464 (1965)

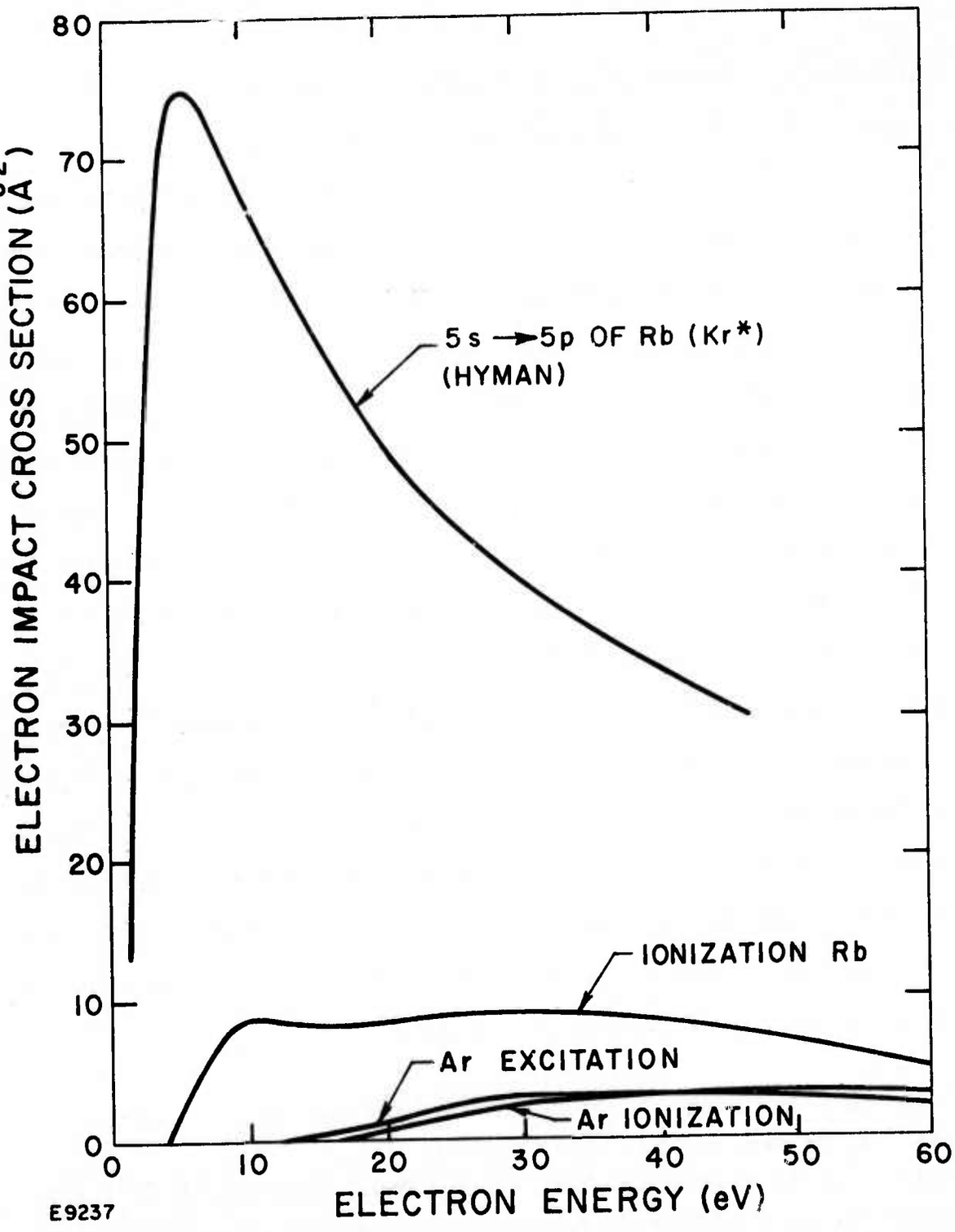

Figure 1 Electron Impact Cross Section for Rb (Kr*) and Ar as a Function of Electron Energy

We have put these cross-sections into a computer code which solves the Boltzmann electron transport equation.[15] This Boltzmann code takes the cross-section data and the electric field and calculates self-consistently the electron energy distribution and the partitioning of discharge energy amongst the various excited states and ionization.[16] The predictions of the code are shown in Figures 2, 3 and 4. Figure 2 shows the percentage of energy that goes into producing Kr^* as a function of the fractional metastable population $Kr^*/(Kr + Ar)$ for electric fields of 2-6 kV/cm atm. It is apparent from Figure 2 that the efficiency of producing the metastables is a strong function of the Kr^* population. For example, the efficiency of forming Kr^* is almost 60% when the fractional population is 10^{-5} and the electric field is 2 kV/cm atm. This efficiency decreases to less than 10% when the fractional population is increased to 10^{-4}. The decrease in efficiency can be made up by increasing the electric field. However, the ionization rate (see Figure 3) rapidly becomes so large that it precludes discharge stabilization by electron attachment (F_2) for cases where the discharge power exceeds the e-beam power into the laser medium. Figure 4 is a plot of the average electron energy as a function of the fractional metastable population. Notice that the electrons cool as the metastable population increases. The cooling effect is much stronger at smaller electric fields.

(15) L.S. Frost and A.V. Phelps, Phys. Rev. 127, 1621 (1962).

(16) The effects of fluorine on the secondary electron distribution have not been included since the electronic impact excitation cross-section is not known. The electron impact cross-sections of F_2 could be large enough to change the predictions of Figures 2, 3 and 4 by as much as 20%. When we ran mixtures of 99.7% Ar and 0.3% O_2, the Boltzmann code predicted 20% of the discharge energy was absorbed by O_2.

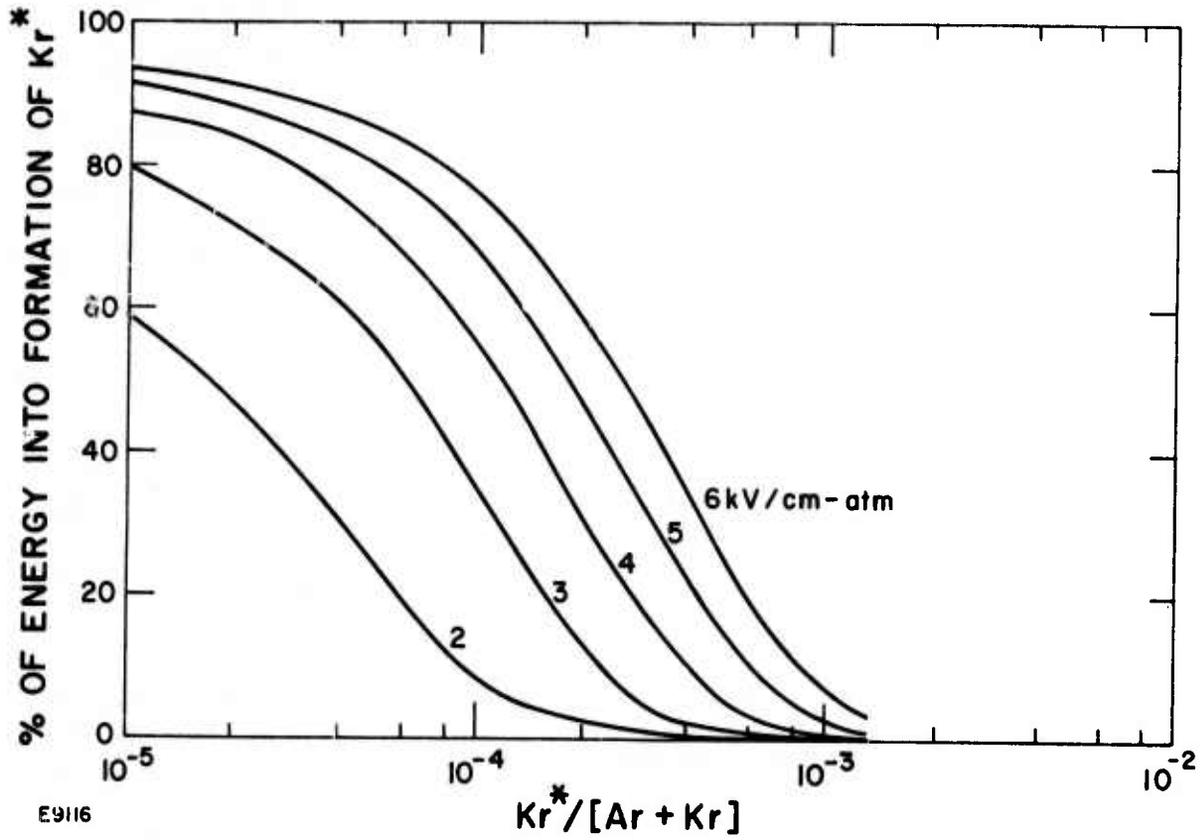

Figure 2 Percentage of Discharge Power into Kr* as a Function of Fractional Kr* Population for Various Applied Electric Fields

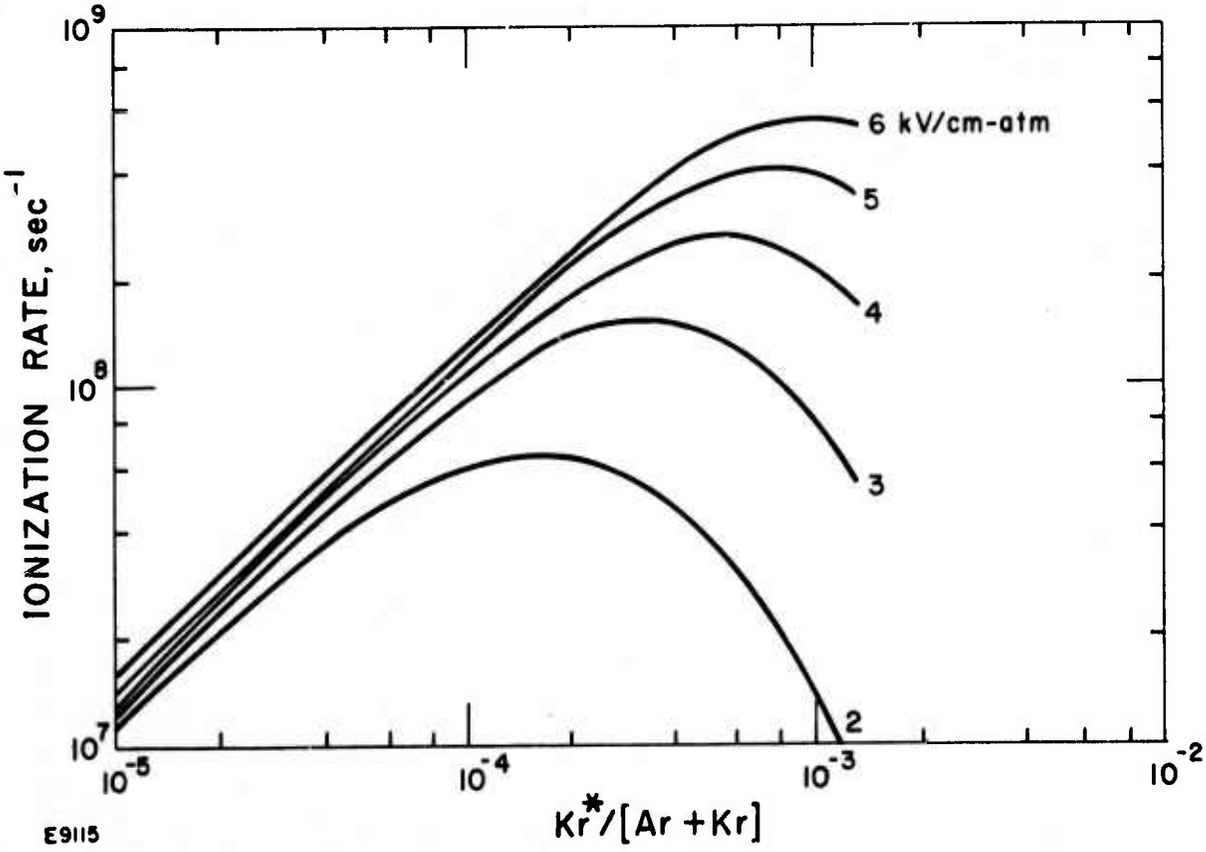

Figure 3 Ionization Rate as a Function of Fractional Kr* Population

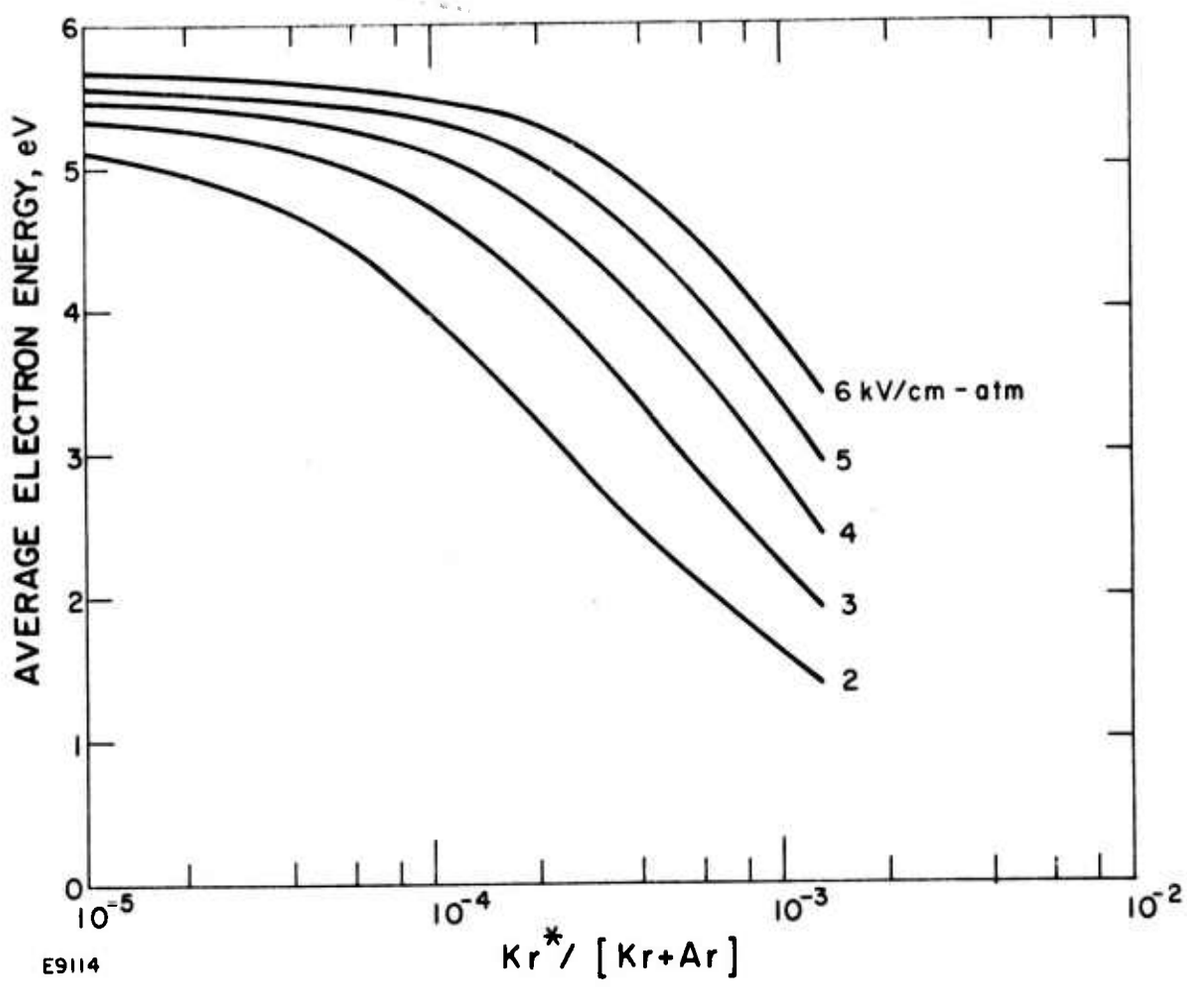

Figure 4 Average Electron Energy as a Function of Fractional Kr* Population

B. DISCHARGE STABILITY

Two equations are important in determining the stability of the discharge in the presence of rapid metastable ionization. The first describes the production and loss of discharge electrons

$$\frac{dn_e}{dt} = S_{eb} + (\nu_i - \beta)\, n_e \tag{1}$$

while the second describes the production and loss of the krypton metastables

$$\frac{dKr^*}{dt} = \langle \sigma v \rangle^* n_e\, Kr - \frac{Kr^*}{\tau_d} \tag{2}$$

In these equations

n_e	=	electron density
S_{eb}	=	electron production rate resulting from the e-beam
ν_i	=	ionization rate
β	=	attachment rate
Kr^*	=	metastable density
$\langle \sigma v \rangle^*$	=	rate constant for production of Kr^* by direct electron impact
Kr	=	ground state Kr density
$(\tau_d)^{-1}$	=	loss rate of metastables (by F_2 to produce KrF^*)

Since metastable ionization dominates ground state ionization by six orders of magnitude at fractional metastable populations of interest,

$$\nu_i = \langle \sigma v \rangle_i\, Kr^* \tag{3}$$

where

$\langle \sigma v \rangle_i$ = metastable ionization rate constant by electron impact.

Under these conditions, Eq. (2) can be rewritten as

$$\frac{d\nu_i}{dt} = A\, n_e - B\nu_i \tag{4}$$

where

$$A = \langle \sigma v \rangle_i \langle \sigma v \rangle^* Kr$$

and (5)

$$B = 1/\tau_d$$

Equations (1) and (4) are a pair of non-linear simultaneous differential equations in n_e and ν_i. If the discharge electric field is constant in time, we can linearize by letting

$$n_e = n_{e0} + n_{e1}(t)$$

and (6)

$$\nu_i = \nu_{i0} + \nu_{i1}(t)$$

The equilibrium electron density n_{e0} and ionization rate ν_{i0} are given by

$$n_{e0} = \frac{S_{eb}}{(\beta - \nu_{i0})} \tag{7}$$

$$\nu_{i0} = A\, n_{e0}/B \tag{8}$$

Equations (7) and (8) can be solved to give

$$n_{e0} = \frac{B\beta}{2A}\left[1 \pm \left\{1 - \frac{4A}{B\beta^2} S_{eb}\right\}^{1/2}\right] \tag{9}$$

and

$$\nu_{i0} = \frac{\beta}{2}\left[1 \pm \left\{1 - \frac{4A}{B\beta^2} S_{eb}\right\}^{1/2}\right] \tag{10}$$

The perturbed electron density n_{e1} and ionization rate ν_{i1} are given by

$$\frac{d\, n_{e1}}{dt} = \nu_{i1}\, n_{e0} + n_{e1}(\nu_{i0}-\beta) \tag{11}$$

and

$$\frac{d\nu_{i1}}{dt} = A\, n_{e1} - B\nu_{i1} \tag{12}$$

Differentiating Eq. (11) w.r.t. time we get

$$\ddot{n}_{e1} = \dot{\nu}_{i1}\, \dot{n}_{e0} + n_{e1}(\nu_{i0}-\beta) \tag{13}$$

Using Eqs. (8), (11) and (12), Eq. (13) reduces to

$$\ddot{n}_{e1} - \dot{n}_{e1}\left[\nu_{i0} - \beta - B\right] + n_{e1}(2\nu_{i0} - \beta)\frac{1}{\tau_d} = 0 \tag{14}$$

From Eq. (14) it is clear that n_{e1} will have temporally decaying solutions if $\beta > 2\nu_{i0}$. When $\beta = 2\nu_{i0}$ one of the roots vanishes and when $\beta < 2\nu_{i0}$, Eq. (14) predicts a temporally growing solution for n_{e1}. So we can conclude that the discharge will be stable if $\beta \geq 2\nu_{i0}$. Going back to Eqs. (9) and (10) it becomes clear that for stable equilibrium we want the negative root, so that for a stable equilibrium,

$$\beta \geq 2\left(\frac{A}{B}\, S_{eb}\right)^{1/2} \tag{15}$$

$$n_{e0} \leq \left(\frac{B}{A}\, S_{eb}\right)^{1/2} \tag{16}$$

$$\nu_{i0} \leq \left(\frac{A}{B}\, S_{eb}\right)^{1/2} \tag{17}$$

We have numerically solved a system of non-linear equations similar to Eqs. (1) and (2). In this analysis we have also included Penning ionization and ionization of the ground state atoms. Figure 5 shows the results of such

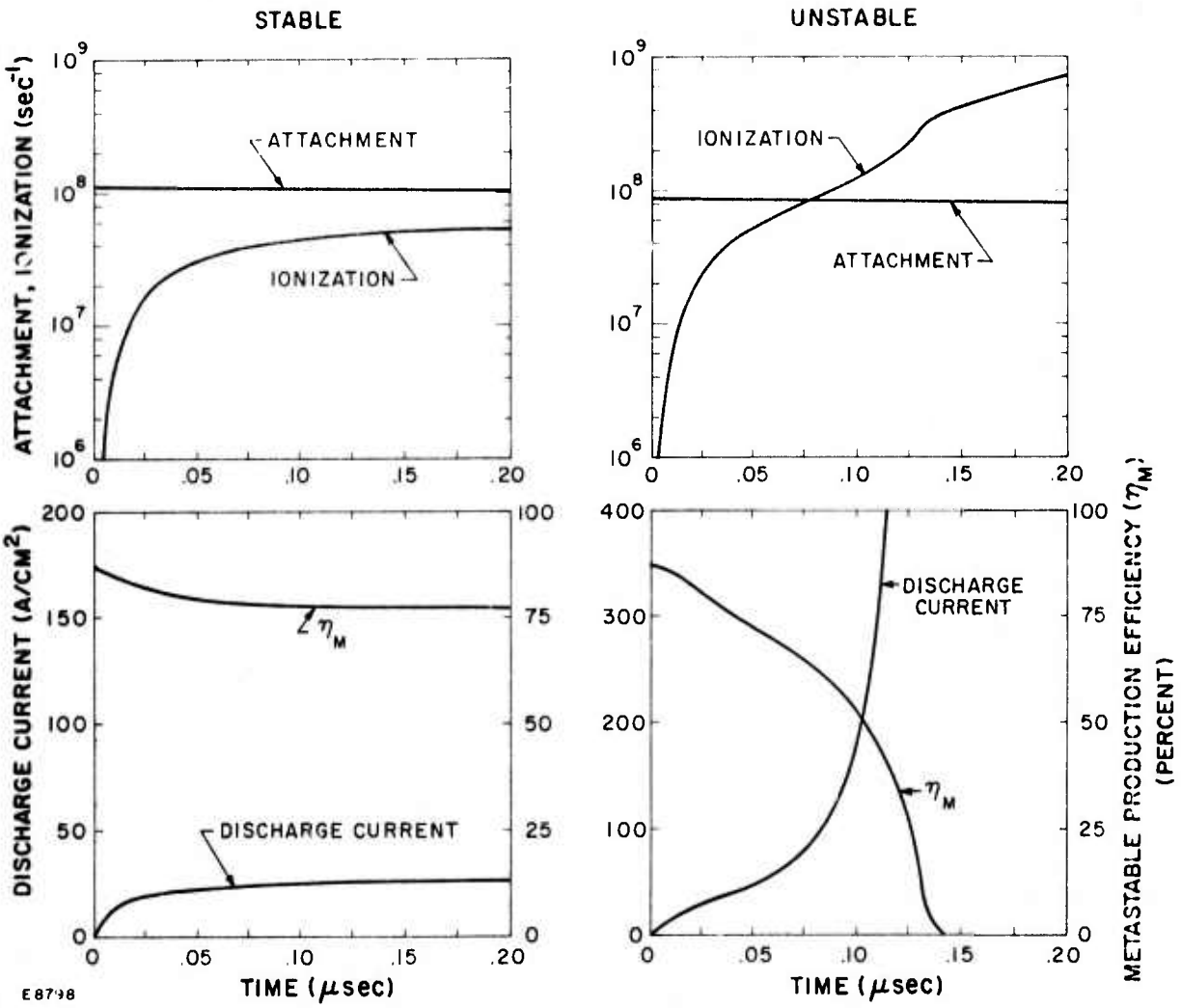

Figure 5 Results of a Numerical Analysis to t System of Equations Similar To Eqs. (1) and (4)

an analysis. On the left-hand side we have the stable discharge condition, i.e., the attachment rate is slightly greater than the equilibrium ionization rate. Notice that the discharge current reaches a constant value asymptotically. Another important feature for the stable discharge case is that the metastable production efficiency η_M remains above 75%. If we keep everything constant but decrease the attachment rate by 20% we observe that the ionization rate increases and after about 70 ns becomes greater than the attachment rate. For this case the discharge current increases faster than exponentially in time.

In Figure 6 we see experimental current, voltage and fluorescence traces for a KrF discharge under stable and unstable operating conditions. The discharge cavity was filled to 2 atm with 0.1% F_2, 2% Kr and 97.9% Ar. Stable discharge conditions were achieved when the 0.3 μF capacitor was charged to 8 kV. Notice that the discharge current reaches a steady state value before the end of the e-beam current pulse. When the capacitor was charged to 10 kV the discharge was unstable. The discharge current increases slowly at first and has a shape very similar to the unstable case shown in Figure 5. The discharge current is volumetrically unstable before it arcs. This assertion is verified if one observes that the fluorescence is increasing for 40 ns subsequent to the onset of rapid current growth.

C. DISCHARGE ENHANCEMENT

In an e-beam controlled discharge one is interested in discharge stability and large ($\geq$5) discharge enhancement. The discharge enhancement is defined here as the ratio between the power deposited in the laser mix by the discharge P_d to the power deposited by the e-beam P_{eb}. This ratio is given by

$$\frac{P_d}{P_{eb}} = \frac{V_D E}{(\beta - \nu_{i0}) E_i} \tag{18}$$

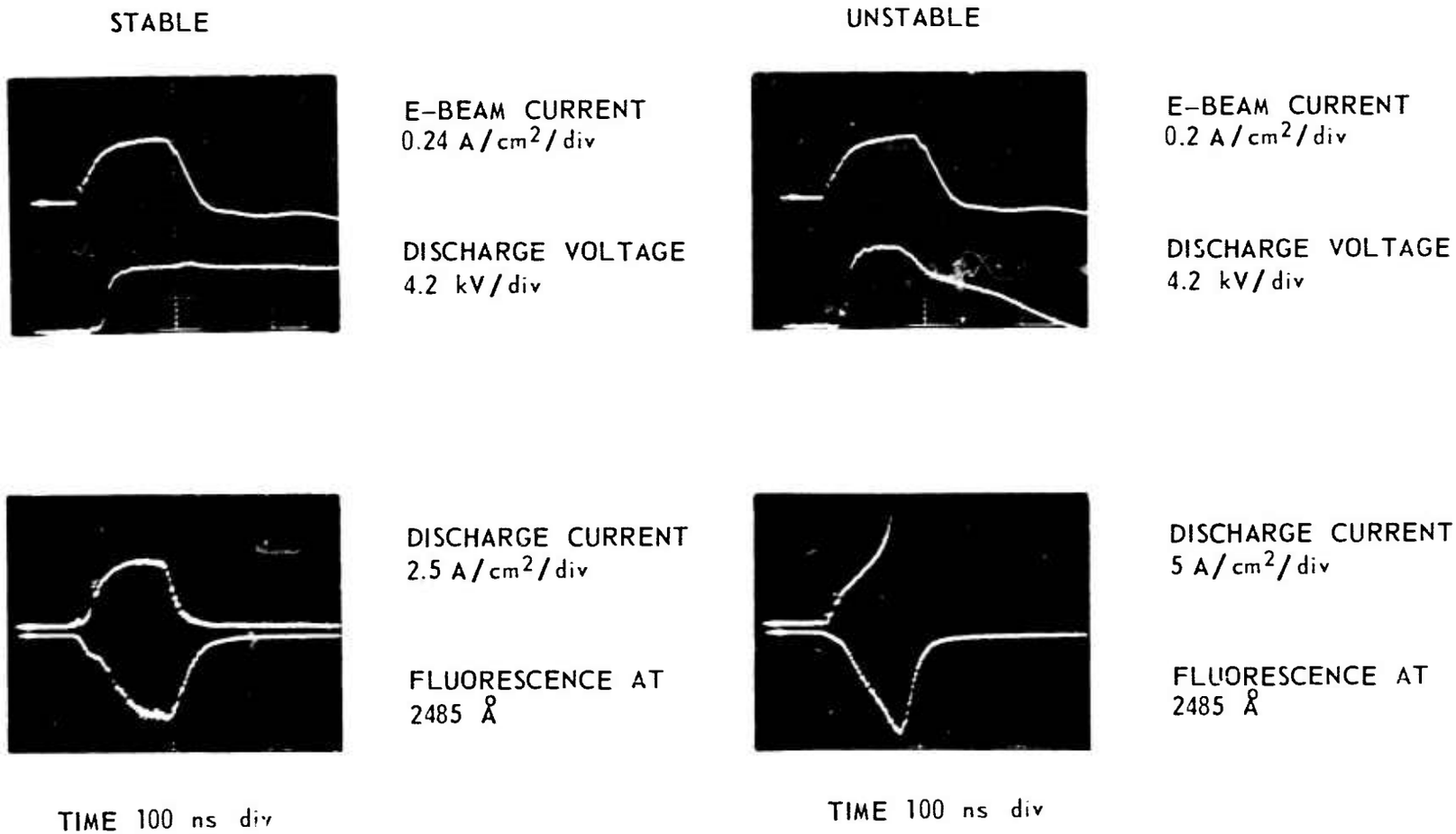

Figure 6 Experimental Data Showing Stable and Unstable Discharge Conditions

where V_D is the discharge electron drift velocity; E is the applied electric field and E_i is the energy required to create an electron-ion pair by the beam electrons. For discharge stability we have shown that $\beta \geq 2\nu_{i0}$, so Eq. (18) can be rewritten as

$$\frac{P_d}{P_{eb}} \leq \frac{V_D E}{\nu_{i0} E_i} \tag{19}$$

Figures 2 and 3 show the predictions of the Boltzmann code for the efficiency of producing metastables, and the ionization rate as a function of the fractional metastable population. With these curves the ionization rate can be expressed as a function of the metastable production efficiency η_M for a given electric field. Thus we can plot the discharge enhancement factor as a function of the metastable production efficiency. Figure 7 shows such a plot for an electric field of 3 kV/cm atm. A result of the analysis is that one can obtain a stable discharge with a large enhancement (> 5) and a large metastable production efficiency (70-80%). However, this is obtained at a price, i.e., the power into the laser mix decreases as one moves along the curve from left to right. It appears reasonable however to obtain discharge enhancement factors of 5-10, metastable pumping efficiencies of 70-80% at a discharge power input of 100 J/liter-atm/μsec.

D. KINETIC DISCHARGE MODEL

Using the rate constants predicted by the Boltzmann code, we have developed a self-consistent kinetics code that follows the temporal evolution of the secondary electrons, positive and negative ions, Ar^*, Kr^* and KrF^*. We couple our kinetics code to a simultaneous set of differential equations that describe the electrical circuit. The outputs of this code include the

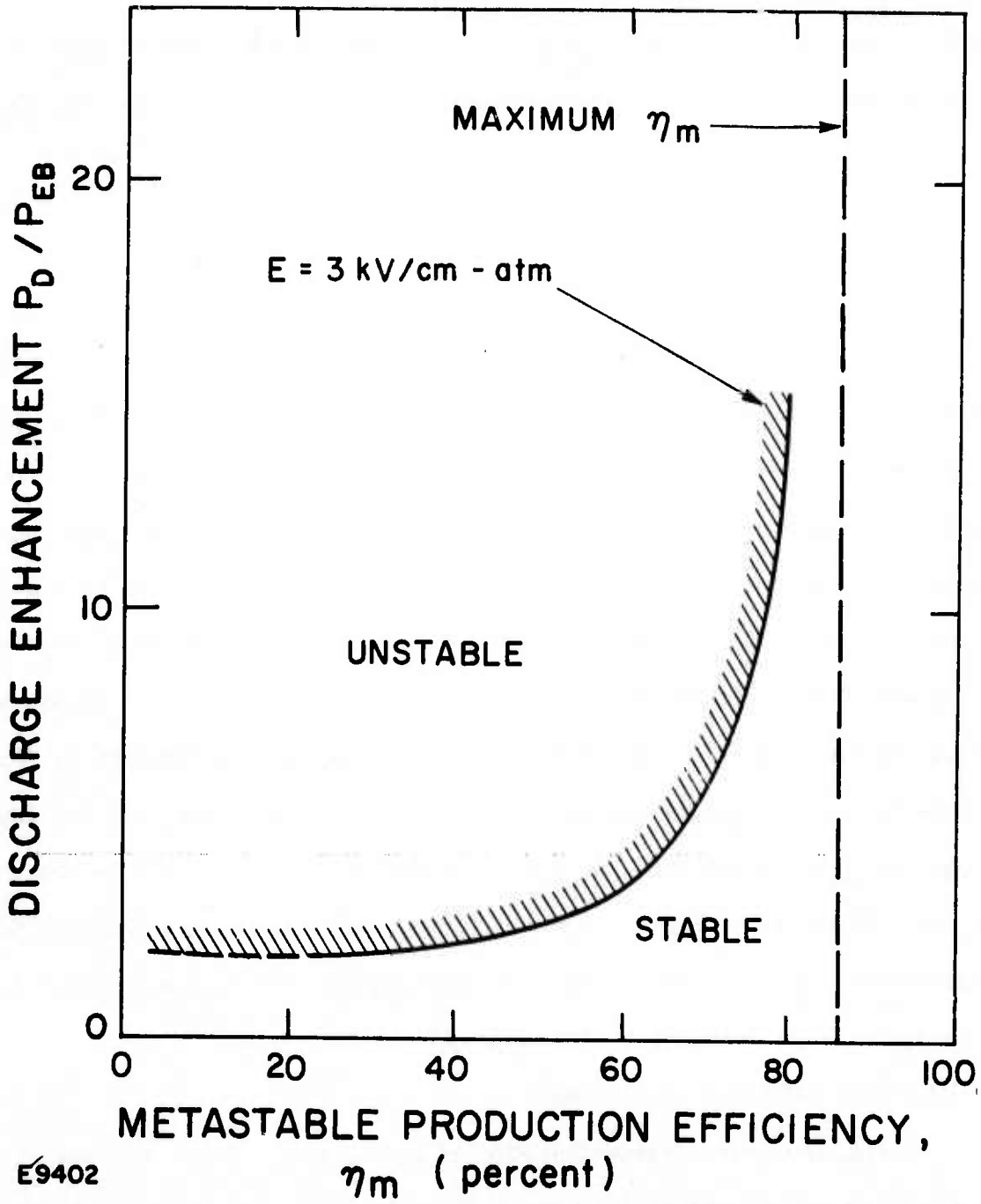

Figure 7 Plot of Discharge Enhancement as a Function of Metastable Production Efficiency for the Limiting Case of a Stable Discharge

temporal evolution of the discharge current and voltage and the KrF^* fluorescence for a given preionization level, discharge capacitor charge voltage and gas mixture.

The predictions of this discharge model have been compared with our KrF laser discharge experiments. The top trace in Figure 8 is the e-beam current in the discharge cavity. The lower trace is the fluorescence as observed by a photomultiplier after the signal passes through a 1/4 meter Jarrel Ash monochromator tuned to 2485 Å. The cavity was filled with a 2 atm mix of 93.7% Ar, 6% Kr and 0.3% F_2. The dashed trace is the prediction of the code. The amplitude of this predicted trace is adjusted to closely match the measured fluorescence. This amplitude normalization was necessary as we did not have an absolute calibration on the fluorescence emanating from the discharge. For subsequent comparisons between experiment and theory no further adjustments were made.

Once the KrF^* fluorescence amplitude was normalized, we measured the magnitude and efficiency of discharge produced KrF^* fluorescence enhancement. Figure 9 shows the experimental results and theoretical predictions when the 0.3 μF capacitor is charged to 10 kV. The top trace is the discharge voltage. The second trace is the discharge current. The third trace is the KrF^* fluorescence. By the end of the pulse the enhancement in the fluorescence is 3. The metastables are being produced with a maximum efficiency of 1.4 times the efficiency of producing the metastables by a pure e-beam. Figure 10 shows the results when the capacitor is charged to 16 kV. In this case the discharge current continually increases until the discharge goes through the glow to arc transition which is marked by an abrupt decrease in KrF^* fluorescence. We believe that the initial

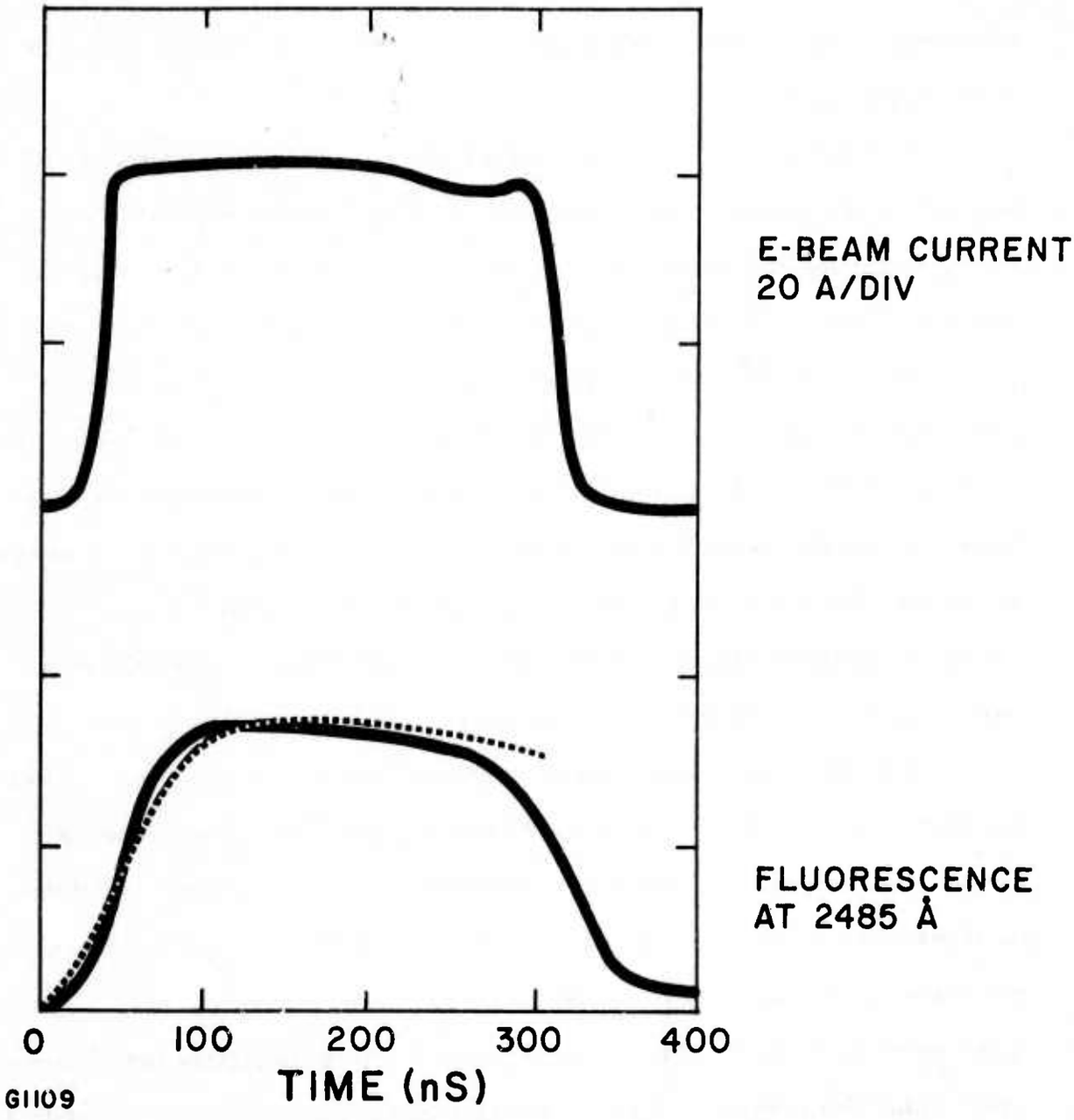

Figure 8 Measured and Predicted Fluorescence for Pure E-Beam Pumping. The discharge cavity contained 2 atm of 93.7% Ar, 6% Kr and 0.3% F_2.

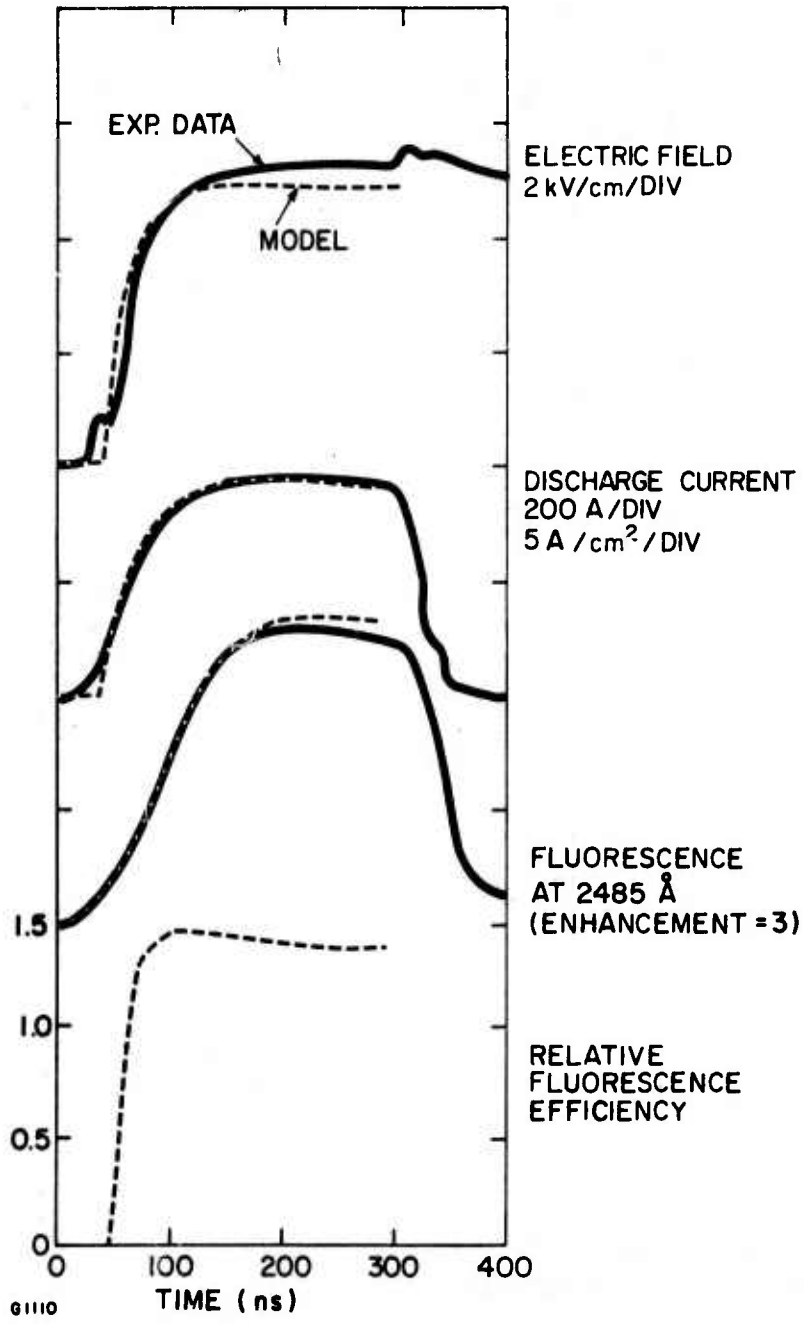

Figure 9 Measured and Predicted Fluorescence when Capacitor is Charged to 10 kV. The discharge cavity contained 2 atm of 93.7% Ar, 6% Kr and 0.3% F_2.

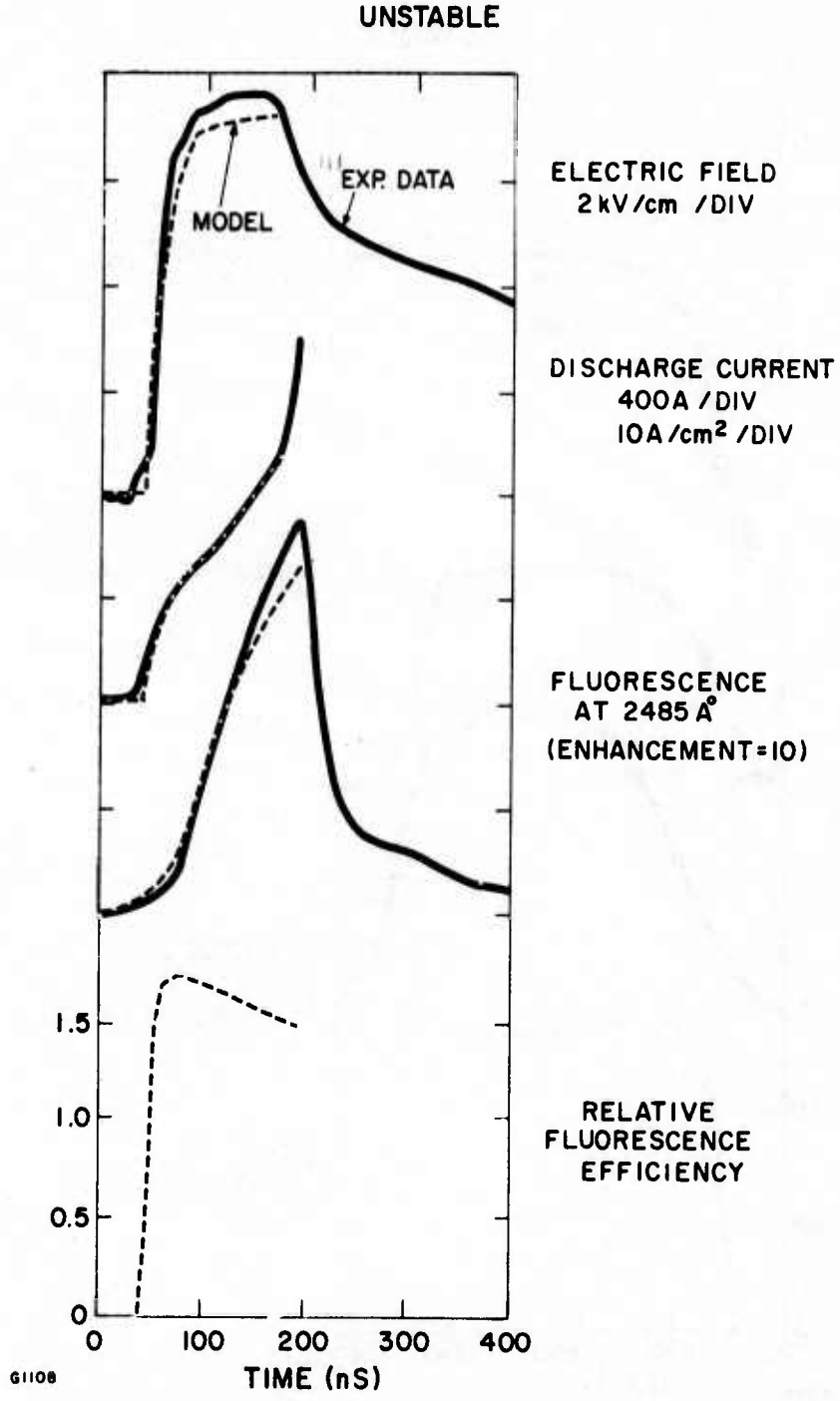

Figure 10 Measured and Predicted Fluorescence when Capacitor is Charged to 16 kV. The discharge cavity contained 2 atm of 93.7% Ar, 6% Kr and 0.3% F_2.

(slow) increase in the discharge current is caused by a volumetric discharge instability discussed previously. The efficiency for producing the metastables rises rapidly to 1.7 times the efficiency of producing metastables in a pure e-beam and then begins to fall despite the fact that the voltage is constant. The KrF^* production efficiency decreases because the metastable density increases and the discharge pumping efficiency of Ar^* and Kr^* falls.

E. CONCLUSIONS

In conclusion, our discharge model predicts that rare gas metastables can be produced with high efficiency (70-80%) as long as the fractional metastable population is kept sufficiently small ($< 2\text{-}3 \times 10^{-5}$). This high metastable production efficiency can lead to KrF^* production efficiencies as high as 35% under carefully controlled discharge conditions. The model also shows that large metastable ionization rates accompany fractional metastable populations of $2\text{-}3 \times 10^{-5}$. In rare gas/halogen mixtures we have shown that this rapid ionization can be balanced by attachment so that long, stable discharge pulses become possible.

REFERENCES

1. J.J. Ewing and C.A. Brau, App. Phys. Lett. 27, 350 (1975).

2. C.A. Brau and J.J. Ewing, App. Phys. Lett. 27, 435 (1975).

3. J.J. Ewing and C.A. Brau, App. Phys. Lett. 27, 350 (1975).

4. J.J. Ewing and C.A. Brau, App. Phys. Lett. 27, 557 (1975).

5. J.A. Mangano and J.H. Jacob, App. Phys. Lett. 27, 495 (1975).

6. J.J. Ewing and C.A. Brau, unpublished.

7. At fractional metastable populations of 10^{-9}, metastable ionization begins to dominate. The metastable production efficiency however is not affected until the fractional population reaches 10^{-5}.

8. The possibility of the excited species having a strong effect on the discharge physics was brought to our attention by P.W. Hoff.

9. In our code we have assumed that excitation of Kr^* to higher lying levels will result in an electron energy loss of 1.6 eV. This assumption is valid if the higher lying levels are rapidly quenched (by three-body processes) back to Kr^*.

10. C.A. Brau and J.J. Ewing, J. Chem. Phys. 63, 4640 (1975).

11. H.Hyman, private communication.

12. R.H. McFarland and J.D. Kinney, Phys. Rev. 137, 1058 (1965).

13. The shape of the total excitation cross-section was obtained from H.S.W. Massey and E.H.S. Bishop, Electronic and Ionic Impact Phenomena, Vol. I, p. 259. To obtain the amplitude of the cross-section we used the Boltzmann code. The amplitude shown in Figure 1 gave the best fit to the first Townsend coefficient that was measured by D.E. Golden and L.H. Fisher, Phys. Rev. 123, 1079 (1961).

14. D. Rapp and P. Englander-Golden, J. Chem. Phys. 43, 1464 (1965).

15. L.S. Frost and A.V. Phelps, Phys, Rev. 127, 1621 (1962).

16. The effects of fluorine on the secondary electron distribution have not been included since the electronic impact excitation cross-section is not known. The electron impact cross-sections of F_2 could be large enough to change the predictions of Figures 2, 3 and 4 by as much as 20%. When we ran mixtures of 99.7% Ar and 0.3% O_2, the Boltzmann code predicted 20% of the discharge energy was absorbed by O_2.

APPENDIX A

TOTAL ELECTRON IMPACT EXCITATION CROSS SECTIONS OF Ar AND Kr

APPENDIX A

TOTAL ELECTRON IMPACT EXCITATION CROSS SECTIONS OF Ar AND Kr

The rare-gas metastables have played an important role in the kinetics of visible and UV lasers. Recently, the use of metastables as an energy reservoir has grown because of the possibility of achieving high-power high-efficiency (≈10%) visible and UV lasers. Initially the energy was pumped into the metastables by high-energy e-beams. The rare-gas excimers[1] were the first lasers built with this pumping method. Subsequently the Ar-N_2 laser was pumped using high-energy beams.[2] More recently, lasing action has been observed in the rare-gas monohalides[3] and the molecular halogens.[4] These lasers have also been pumped by e-beam-controlled discharges[5] and avalanche discharges.[6] By discharge

(1) H.A. Koehler, L.J. Ferderber, D.L. Redhead, and D.J. Ebert, Appl. Phys. Lett. 21, 198 (1972); P.W. Hoff, J.C. Swingle, and C.K. Rhodes, ibid. 23, 245, (1973).

(2) Stuart K. Searles and G.A. Hart, Appl. Phys. Lett. 25, 79 (1974); Earl R. Ault. Mani L. Bhaumik, and N. Thomas Olson, IEEE J. Quantum Electron. QE-10, 624 (1974).

(3) C.A. Brau and J.J. Ewing, Appl. Phys. Lett. 27, 435 (1975); J.J. Ewing and C.A. Brau, ibid. 27, 350 (1975); S.K. Searles and G.A. Hart, ibid. 27, 243 (1975); E.R. Ault, R.S. Bradford, and M.L. Bhaumik, ibid. 27, 413 (1975).

(4) J.J. Ewing and C.A. Brau, Appl. Phys. Lett. 27, 557 (1975); J.R. Murray, J.C. Swingle, and G.E. Turner, Jr., ibid. 28, 530 (1976).

(5) J.A. Mangano and J.H. Jacob, Appl. Phys. Lett. 27, 495 (1975); J.J. Ewing, J.H. Jacob, J.A. Mangano, and H.A. Brown, ibid. 28, 656 (1976).

(6) R. Burnham, D. Harris and N. Djeu, Appl. Phys. Lett. 28, 86 (1976); D.C. Sutton, S.H. Suchard, D.L. Gibb, and G.P. Wang, ibid. 28, 522 (1976).

pumping the rare-gas metastables are excited by secondary electrons. For a detailed knowledge of the laser kinetics and excited state populations, the electron impact cross sections should be known to accuracies of 20% and better.[7, 8]

In this letter we describe a method of accurately determining the magnitude of the total excitation cross sections of Ar and Kr. The procedure depends on knowing the electron impact ionization cross section of the rare gas and the first Townsend coefficient. As we will show subsequently, a 30% change in the magnitude of the metastable cross section results in a change of 2-3 in the first Townsend coefficient. The ionization cross sections of the rare gases have been measured by Rapp and Englander-Golden.[9] The absolute magnitude of the electron impact cross section of Ar was first measured by Maier-Leibnitz.[10] Using a similar apparatus, Schaper and Scheibner[11] have, more recently, measured the electron excitation cross section in the rare gases. For the special case of Ar the cross section measured by Shaper and Scheibner is a factor of 2 smaller than Maier-Leibnitz's measurement. The shape of the electron impact cross section obtained by Olmsted et al.[12] is similar to that of Schaper and Scheibner.

---

(7) J.D. Daugherty, J.A. Mangano, and J.H. Jacob, Appl. Phys. Lett. 28, 581 (1976).

(8) J.H. Jacob and J.A. Mangano, Appl. Phys. Lett. 28, 724 (1976).

(9) D. Rapp and P. Englander-Golden, J. Chem. Phys. 43, 1464 (1965).

(10) H. Maier-Leibnitz, Z. Phys. 95, 499 (1935).

(11) M. Schaper and H. Scheibner, Beit. Plasma Phys. 9, 45 (1969).

(12) J. Olmsted, A.S. Newton, and I.E. Street, J. Chem. Phys. 42, 2321 (1965).

The first Townsend coefficient in the rare gases has been measured by Kruithof and Penning[13] (KP). Golden and Fisher[14] (GF) have carefully investigated the first Townsend coefficient α in argon. They have obtained, for $E/P \leq 7$ V cm^{-1}/mm of Hg, values of α that are considerably less than those of KP. Figure A-1 shows the results of KP and GF. The results of GF are represented by a dashed curve at low E/P because at these E/P values they found that α was a strong function of the electrode spacing. At the larger values of E/P the dependency of α was a much weaker function of electrode spacing. At an E/P of 5 V cm^{-1}/mm of Hg, there is an order-of-magnitude difference between the two measurements. For E/P greater than 8 V cm^{-1}/mm of Hg, the two measurements agree to better than 10%.

Also shown in Figure A-1 are the predictions of the AERL Boltzmann code. For these results we have used the ionization cross section as measured by Rapp and Englander-Golden.[9] When the excitation cross section of Schaper and Scheibner[11] is used, the predicted α/P is about 30% larger than the measured values when $E/P > 7$ V cm^{-1}/mm of Hg. If the Schaper and Scheibner cross sections are increased by 10%, the predicted and measured values agree to $\pm$10% for $E/P > 8$ V cm^{-1}/mm of Hg. For $E/P \leq 8$ V cm^{-1}/mm of Hg, the predicted values are in closer agreement with the measurement of GF than with the measurement of KP. Finally, in Figure A-1 we also see the predicted α/P when the electron impact cross sections of Eggarter[15] are used. Figure A-2 shows the electron impact cross sections

(13) A.A. Kruithof and F.M. Penning, Physica (Hague) 3, 515 (1936).
(14) D.E. Golden and L.H. Fisher, Phys. Rev. 123, 1076 (1961).
(15) E. Eggarter, J. Chem. Phys. 62, 833 (1975).

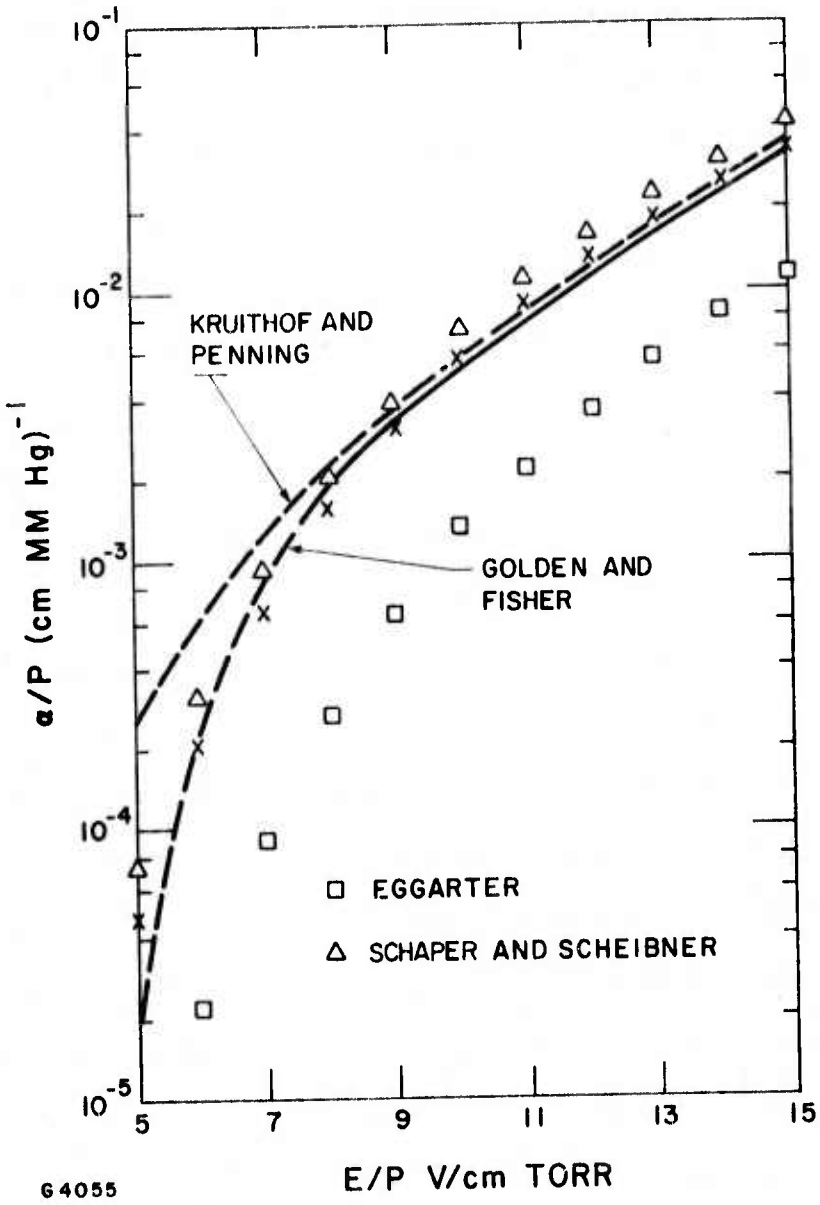

Figure A-1 Curves Showing the Experimental and Predicted Values of the First Townsend Coefficient α as a Function of E/P. The experimental results of Kruithof and Penning agree to within 10% with the results of Golden and Fisher for $E/p \geq 9$ V/cm cm Torr. Also shown are the predicted values of α/p when Shaper and Scheibner, and Eggarter, cross sections are used. The crosses are the predicted values of α /p when Shaper and Scheibner's measurement is increased by 10%.

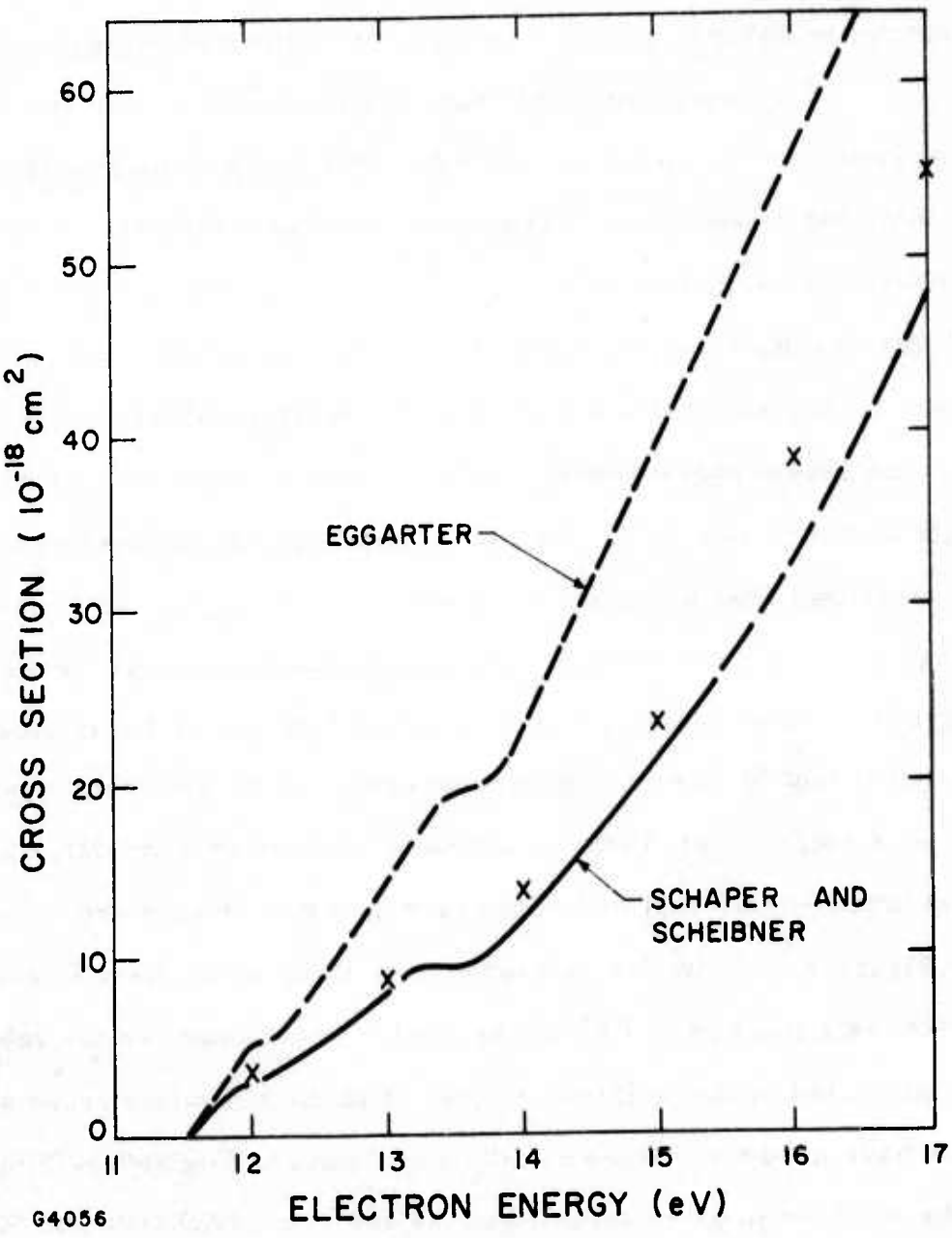

Figure A-2 Electron Excitation Cross Sections for Argon as Measured by Shaper and Scheibner (solid curve). The dashed curve is the cross-section recommended by Eggarter. The crosses are about 10% larger than the measurements of Shaper and Scheibner and result in the best fit of the predicted to the measured first Townsend coefficient.

as measured by Schaper and Scheibner and the values recommended by Eggarter. Also shown is the total cross section that gives the best fit to the measured first Townsend coefficient. This cross section is about 10% larger than that measured by Schaper and Scheibner; however, it changes the predicted value of α by 30%.

The results shown in Figure A-1 for the predicted values of the first Townsend coefficient have assumed that the electron energy loss is 11.55 eV, which is the lowest excited energy level of argon. There are, of course, a manifold of 4p and 4s states. We have attempted to model these on the computer. This was done by having the same ratio of σ_{4p}/σ_{4s} as Eggarter.[15] However, the total cross section used was the same as shown by the crosses in Figure A-2. The difference in the predicted values of α was only 5%. So it appears that for the rare gases one can treat the electron impact cross section as a single level. This is fortunate because detailed data on the electron impact cross sections of the rare-gas metastables are not available.

Figure A-3 shows the measurements of KP of the first Townsend coefficient as a function of E/P for krypton. Also shown are the values of α/P as predicted by the Boltzmann code. For the ionization cross section of Kr we have used the measured values of Rapp and Englander-Golden.[9] When the electron impact excitation cross sections of Schaper and Scheibner[11] are used, the predicted values of α/P are 10% smaller than the measured values for an E/P of $\geq$9 V cm^{-1}/mm of Hg. If Shaper and Scheibner's cross section is decreased by 3%, the predicted and measured values of α/P are in much closer agreement for larger values of E/P. As in the case of Ar when the E/P < 9 V cm^{-1}/mm of Hg, the measured and predicted values of α/P are considerably different. At an E/P of 5 V cm^{-1}/mm of Hg, for example, the difference is almost in order of magnitude.

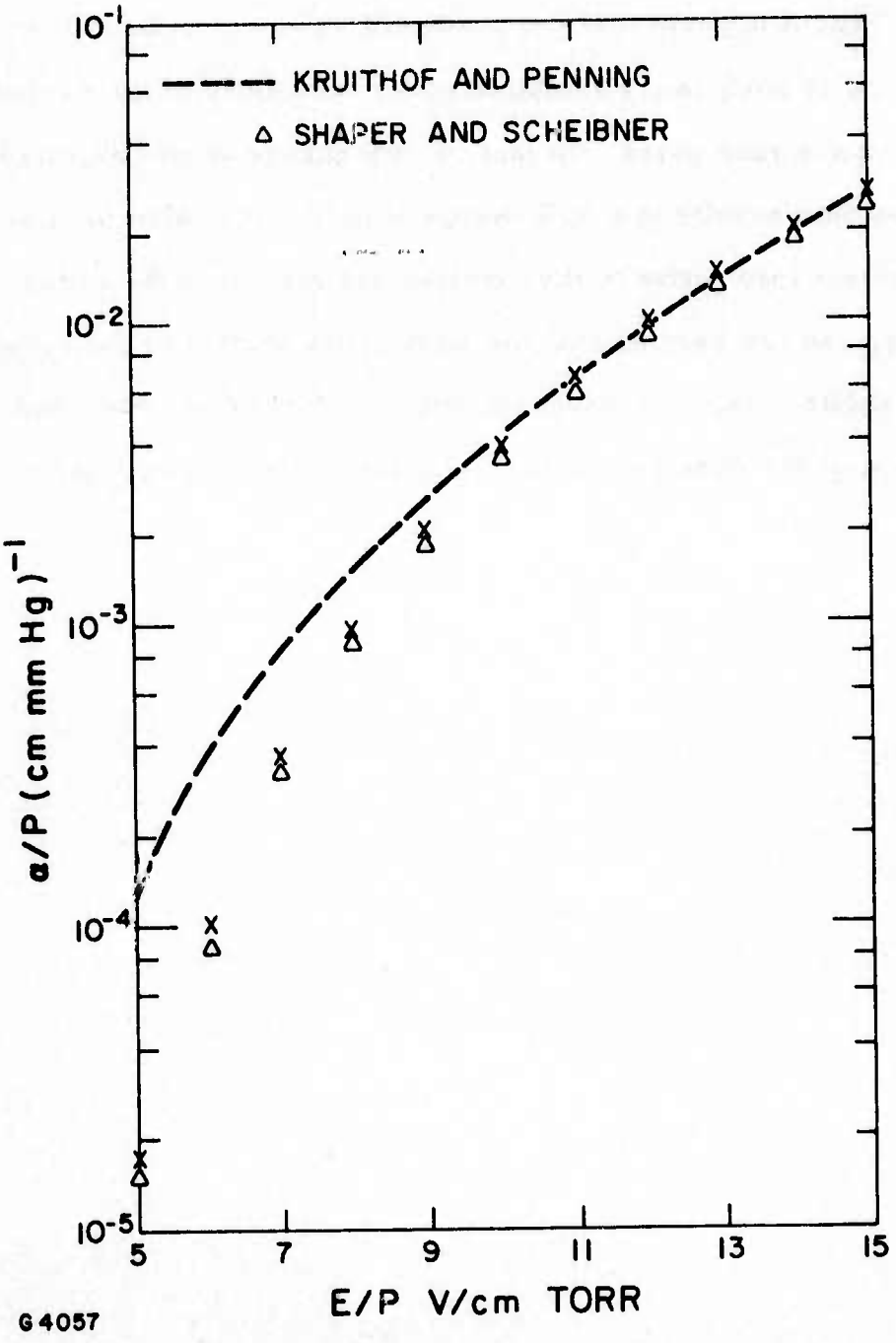

Figure A-3 Same as Figure A-1 Except That the Gas in Question is Krypton. The crosses are the predicted first Townsend coefficient when Shaper and Scheibner's measurements are decreased by 3%.

Thus it appears that the predicted value of the first Townsend coefficient is sufficiently sensitive to the magnitude of the excitation cross section of the rare gases. In fact, a 10% change in the magnitude of the cross section results in a 30% change in α/P. It is also fortunate that α/P is relatively insensitive to the detailed assignment of the cross section. As a result, one can assume that the total cross section is the result of the lowest excited state. It would be valuable if more accurate and recent measurement of the first Townsend coefficient were available for the rare gases.

APPENDIX A

REFERENCES

(1) H. A. Koehler, L. J. Ferderber, D. L. Redhead, and D. J. Ebert, Appl. Phys. Lett. 21, 198 (1972); P. W. Hoff, J. C. Swingle, and C. K. Rhodes, ibid. 23, 245, (1973).

(2) Stuart K. Searles and G. A. Hart, Appl. Phys. Lett. 25, 79 (1974); Earl R. Ault. Mani L. Bhaumik, and N. Thomas Olson, IEEE J. Quantum Electron. QE-10, 624 (1974).

(3) C. A. Brau and J. J. Ewing, Appl. Phys. Lett. 27, 435 (1975); J. J. Ewing and C. A. Brau, ibid. 27, 350 (1975); S. K. Searles and G. A. Hart, ibid. 27, 243 (1975); E. R. Ault, R. S. Bradford, and M. L. Bhaumik, ibid. 27, 413 (1975).

(4) J. J. Ewing and C. A. Brau, Appl. Phys. Lett. 27, 557 (1975); J. R. Murray, J. C. Swingle, and G. E. Turner, Jr., ibid. 28, 530 (1976).

(5) J. A. Mangano and J. H. Jacob, Appl. Phys. Lett. 27, 495 (1975); J. J. Ewing, J. H. Jacob, J. A. Mangano, and H. A. Borwn, ibid. 28, 656 (1976).

(6) R. Burnham, D. Harris and N. Djeu, Appl. Phys. Lett. 28, 86 (1976); D. C. Sutton, S. H. Suchard, D. L. Gibb, and G. P. Wang, ibid. 28, 522 (1976).

(7) J. D. Daugherty, J. A. Mangano, and J. H. Jacob, Appl. Phys. Lett. 28, 581 (1976).

(8) J. H. Jacob and J. A. Mangano, Appl. Phys. Lett 28, 724 (1976).

(9) D. Rapp and P. Englander-Golden, J. Chem. Phys. 43, 1464 (1965).

(10) H. Maier-Leibnitz, Z. Phys. 95, 499 (1935).

(11) M. Schaper and H. Scheibner, Beit. Plasma Phys. 9, 45 (1969).

(12) J. Olmsted, A. S. Newton, and I. E. Street, J. Chem. Phys. 42, 2321 (1965).

(13) A. A. Kruithof and F. M. Penning, Physica (Hague) 3, 515 (1936).

(14) D. E. Golden and L. H. Fisher, Phys. Rev. 123, 1076 (1961).

(15) E. Eggarter, J. Chem. Phys. 62, 833 (1975).

APPENDIX B

TOWARD EFFICIENT EXCIMER LASERS

APPENDIX B

TOWARD EFFICIENT EXCIMER LASERS

An e-beam can drive mixture of rare gases and halogens to lase at high powers in the visible and ultraviolet, (see Table B-1) but the efficiency decreases as e-beam power increases. E-beams can be eliminated with avalanche-discharge pumping, but at a sacrifice in power. To achieve both high power and efficiency, the two pumping methods must be combined.

The discovery of rare-gas-monohalide[1-6] and molecular-halogen[7-9] lasers led rapidly to development of krypton- and argon-fluoride systems capable of producing 100-joule pulses under direct excitation by e-beams.[10] To date the highest laser efficiency achieved by e-beam pumping of rare-gas monohalide is 15%.[11, 12] Although the molecular halogens (Br_2, I_2) have high fluorescence efficiencies, laser efficiency greater than 1% has yet to be achieved. These lasers have the potential of achieving over-all efficiencies as high as 15%.

(1) J. J. Ewing and C. A. Brau, Phys. Rev., A12, 129 (1975).

(2) J. E. Velazco and D. W. Setser, J. Chem. Phys., 62, 1990 (1975).

(3) C. A. Brau and J. J. Ewing, Appl. Phys. Lett. 27, 435 (1975).

(4) J. J. Ewing and C. A. Brau, Appl. Phys. Lett. 27, 350 (1975).

(5) S. K. Searles and G. A. Hart, Appl. Phys. Lett. 27, 243 (1975).

(6) E. R. Ault, R. S. Bradford and M. L. Bhaumik, Appl. Phys. Lett. 27, 413 (1975).

(7) M. V. McCusker et al, Appl. Phys. Lett. 27, 363 (1975).

(8) J. J. Ewing and C. A. Brau, Appl. Phys. Lett., 27, 557 (1975).

(9) J. R. Murray, J. C. Swingle and G. E. Turner, Jr., Appl. Phys. Lett. 28, 530 (1976).

(10) J. M. Hoffman, A. K. Hays, and G. C. Tisone, Appl. Phys. Lett. 28, 538 (1976).

(11) M. L. Bhaumik, R. S. Bradford, Jr. and E. R. Ault, Appl. Phys., Lett 28, 23 (1976)

(12) C. A. Brau and J. J. Ewing (unpublished)

TABLE B-1. CANDIDATE MOLECULES FOR VISIBLE AND UV LASERS

Molecule	Wavelength (nm)	E-beam Pumping	Discharge Pumping E-beam Control	Avalanche
XeBr	282	X		
XeCl	308	X		
XeF	352	X	X	X
KrCl	222	X		
KrF	249	X	X	X
ArF	192	X		
I_2	342	X	X	
Br_2	292	X	X	

1. CONTROLLED VS AVALANCHE PUMPING

Discharge pumping of rare-gas monohalide and halogen lasers was first demonstrated at Avco-Everett.[13, 14] Most, but not all, the discharge electrons were produced by a high-energy e-beam. The discharge which provided most of the pump power was then run in the ionization produced by the e-beam.

Avalanche discharges were used subsequently to pump rare-gas monohalides at both the Naval Research Laboratory and the Aerospace Corp.[15, 16] Instead of controlling ionization with an e-beam, this method preionizes the laser medium with ultraviolet radiation. The electrons freed by photo-ionization rapidly form negative halogen ions

$$e + X_2 \rightarrow X^- + X$$

The negative ions then provide an easily ionizable source for production of discharge electrons.[17] Electron detachment presumably occurs by discharge-electron impact and laser-photon detachment. The negative ions which are lost by recombination result in a more uniform spatial distribution. When the discharge electric field is applied, the electron density avalanches rapidly by several orders of magnitude, and large discharge-energy inputs are possible.

An avalanche discharge yields higher pulse-repetition rates and is simpler than other pump methods, so it should have wide application in isotope separation and other photochemical processes which require pulses of

(13) J.A. Mangano and J.H. Jacob, Appl. Phys. Lett. 27, 495 (1975).

(14) J.J. Ewing, H.H. Jacob, J.A. Mangano, and H.A. Brown, Appl. Phys. Lett. 28, 581 (1976).

(15) R. Burnham, D. Harris and N. Djeu, Appl. Phys. Lett. 28, 86 (1976).

(16) D.G. Sutton, S.N. Suchard, O.L. Gibb, and C.P. Wang, Appl. Phys. Lett. 28, 522 (1976).

(17) Jim Hsia, Avco-Everett Research Laboratory, private communication.

one joule or less. But avalanche pumping exacerbates the effects of discharge nonuniformities, limiting the power and pulse lengths attainable. If the lower laser level does not bottleneck the laser transition - and for many excimer lasers it does not - the controlled-discharge technique gives much higher average power than the avalanche approach.

2. COMPARING OVER-ALL EFFICIENCIES

For two reasons, the controlled discharge is more efficient than direct e-beam or avalanche pumping. Controlled discharges are more efficient at producing the rare-gas metastables through which pump power is channeled to the upper laser level. E-beam control permits stable discharge pulses to maintain excited-state populations at optimum levels for a microsecond or longer. Our studies show that a controlled discharge can be 1.5 times more efficient in producing the upper laser level than direct e-beam pumping.[18]

In contrast, no method of stabilizing an avalanche discharge is available and excited-state populations cannot be maintained at the optimum level for a significant portion of the discharge pulse. Consequently, for excited-state populations higher than optimum, the processes of metastable excitation and ionization reduce the metastable-production efficiency. Overall efficiency is also limited by photon absorption due to large excited-state populations and by electron quenching of excited states which can accompany electron avalanches. For excited state populations lower than optimum, the reduced small-signal gain implies lower efficiency in extracting laser power.

(18) J.H. Jacob and J.A. Mangano Appl. Phys. Letts. 28, 724 (1976).

3. STABILIZING AND ENHANCING DISCHARGES

Another advantage of e-beam control is more efficient coupling of electrical power into the laser medium than with pure e-beam or avalanche approaches. With suitable pulse-forming networks, about 90% of electrical power can be coupled efficiently to the nearly constant impedance of a controlled discharge. In pure e-beam pumping, energy losses in the foil and the support structure limit the over-all system efficiency; in an avalanche discharge, the order of magnitude changes in discharge impedance severely limit the efficiency with which electrical energy can be coupled into the laser mix.

The keys to realizing the advantages of e-beam control are discharge stability and the degree of discharge enhancement - the ratio of discharge power to e-beam power. We have found that for gas mixtures typical of these lasers, rapid metastable ionization can be balanced by electron attachment to maintain discharge stability. Further, stability can be maintained with both large enhancement ratios and high-efficiency of production of metastables and excimers.[18, 19] Achieving the best balance between efficiency and output power, however, will require more detailed knowledge of the kinetics of pumping reactions.

In rare-gas monohalide lasers the highest efficiencies have been obtained using argon as the buffer gas. In KrF the optimum mix contains no more than 15% Kr and in xenon fluoride no more than 1% Xe. A possible explanation is that Kr and Xe quench the upper laser level at a gas kinetic rate.

(19) J.D. Daugherty, J.A. Mangano, and J.H. Jacob, Appl. Phys. Lett. 28, 581 (1976).

In e-beam-controlled pumping of the KrF* laser, argon atoms are first ionized by high-energy electrons $\vec{e}$

$$\vec{e} + Ar \rightarrow Ar^+ + e + \vec{e} \qquad \text{(B-1)}$$

The secondary electrons e gain energy in the applied electric field and most of the discharge energy initially goes into producing argon metastables, Ar^*

$$\vec{e} + Ar \rightarrow Ar^* + e \qquad \text{(B-2)}$$

These metastables are very reactive and can have numerous exit channels. At pressures below 3 atmospheres the most probable reaction is

$$Ar^* + F_2 \rightarrow ArF^* + F \qquad \text{(B-3)}$$

Reaction (B-3) proceeds with a rate constant of 7×10^{-10} cubic centimeter per second and ArF* is formed with a unit branching ratio.[20] Other possible reactions, especially at higher pressures, are

$$Ar^* + 2Ar \rightarrow Ar_2^* + Ar \qquad \text{(B-4)}$$

and

$$Ar^* + Ar + Kr \rightarrow ArKr^* + Ar \qquad \text{(B-5)}$$

The rate constant for reaction (B-4) is about 2×10^{-32} cm^6/sec.[21] Unfortunately, the rate for reaction (B-5) has not yet been measured. However, because 10 times more argon than krypton is used, the rate will have to be about 2×10^{-31} cm^6/sec to compete with reaction (B-4). The rate will have to be about 10^{-30} cm^6/sec if it is to compete with reaction (B-3), so

(20) J.E. Velazco, J.H. Kolts and D.W. Setser (unpublished)

(21) See for example M. Bourene, O. Dutuit and J. LeCalve, J. Chem. Phys. 63, 1668 (1975).

clearly it is of prime importance to know the reaction rate for (B-5) if the detailed kinetic chain for KrF^* formation is to be understood.

4. FORMING THE UPPER LASER LEVEL

The upper laser level is then formed by one of the displacement reactions

$$ArF^* + Kr \rightarrow KrF^* + AR \qquad \text{(B-6)}$$

and

$$ArKr^* + F_2 \rightarrow KrF^* + F + Ar \qquad \text{(B-7)}$$

The detailed kinetic chain will depend of course on the rates of reactions (B-5) and (B-6). We have measured KrF^* production efficiencies of 30% to 35%; such efficiencies are only possible if the KrF^* is formed from Ar^* with almost unit branching ratio.

In molecular-halogen laser - the bromine laser for example - the reaction equivalent to (B-3) is

$$Ar^* + Br_2 \rightarrow Ar + Br^* + Br \qquad \text{(B-8)}$$

Gundel et al[22] have established that Br_2 quenches Ar^* with a rate constant of 6.5×10^{-10} cm^3/sec and Br^* is formed with a branching ratio 0.98. The radiative lifetime of Br^* is short but at high pressures the radiation is trapped, so excited bromine atoms give up their energy to Br_2 to form the upper laser level

$$Br^* + Br_2 \rightarrow Br_2^* + Br \qquad \text{(B-9)}$$

There are, of course, reactions that result in inefficiencies. The metastables probably have large electron-impact crosssection to higher lying levels Ar^{**}

$$e + Ar^* \rightarrow Ar^{**} + e \qquad \text{(B-10)}$$

(22) L.A. Gundel et al (unpublished)

Further, the ionization rate is greatly enhanced because of the ionization of the metastables

$$e + Ar^* \rightarrow Ar^+ + 2e \qquad \text{(B-11)}$$

Fortunately this rapid ionization can be balanced by electron attachment

$$e + F_2 \rightarrow F^- + F \qquad \text{(B-12)}$$

therefore stabilizing the discharge.

For the remainder of this article we will discuss the physics of the KrF^* laser, because its discharge has been modeled in the greatest detail. However, the physics of other rare-gas monohalides and halogen discharges will be similar. The discharge physics is strongly affected by electron-impact excitation and by ionization of the rare-gas metastables. To model these effects we have treated the krypton metastable as rubidium and the argon metastable as potassium, an analogy used successfully in predicting the emission spectra of excited rare-gas monohalides.

Some of the electron-impact cross sections used in our model are shown in Figure B-1. The cross section for excitation from the 5s configuration to the 5p configuration in Rb (Kr^*) has a peak value of 75 square angstroms at 8 electronvolts. Also shown are the ionization cross section of Rb and the excitation and ionization cross sections of Ar. From Figure B-1 it is clear that the peak value of the metastable-excitation cross section is 30 times the peak value of the argon-excitation cross section. More important, however, is the ability of most of the electrons to excite the 5s- to- 5p transitions - which have a threshold of 1.6 eV - but only the high-energy tail of the electron-energy distribution can produce metastables from the ground state.

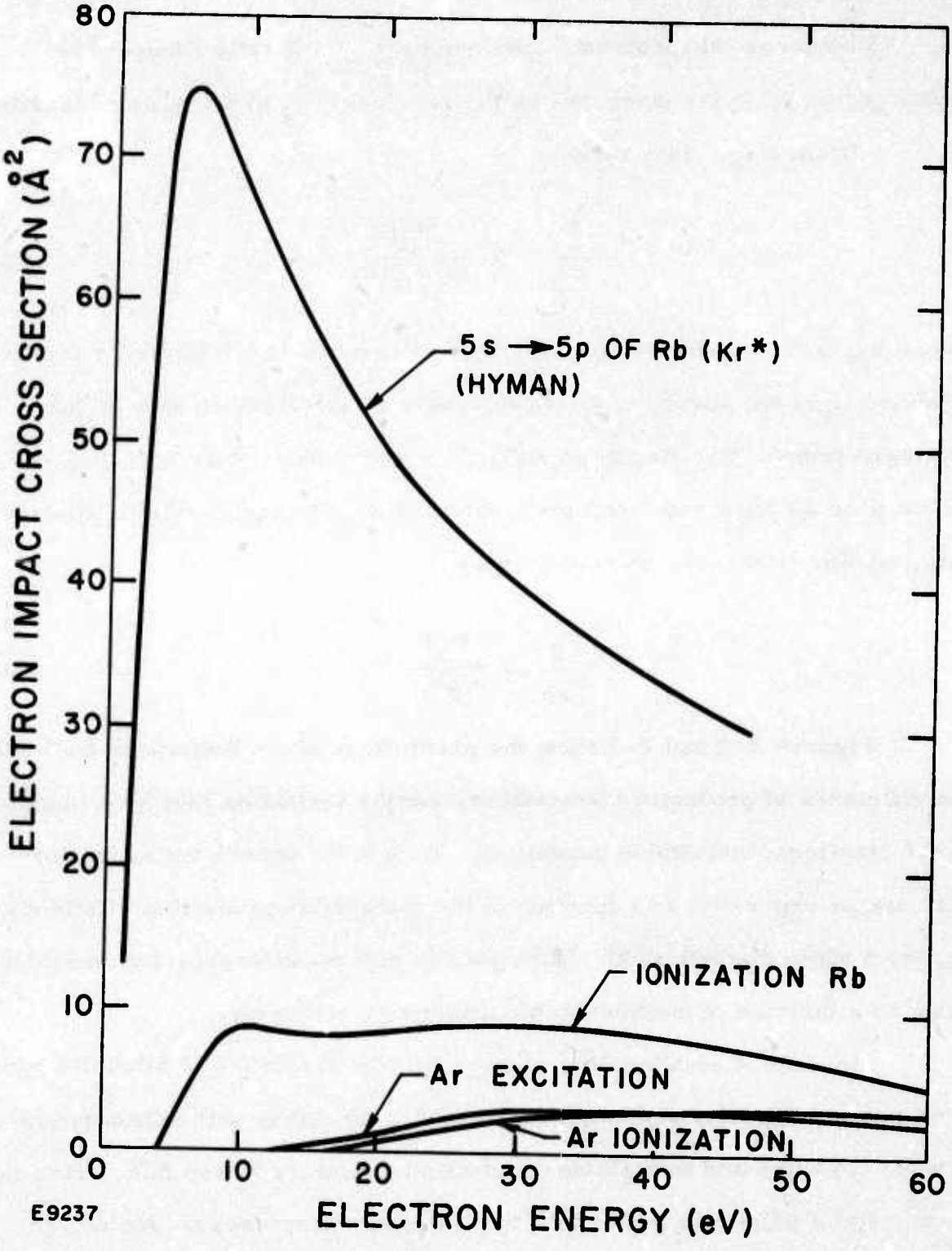

Figure B-1 Electron-Impact Crossections of Rubidium (Krypton Equivalent) and Argon as Functions of Electron Energy

Discharge enhancement is defined here as the ratio between the power deposited in the laser mix by the discharge P_d to the power deposited by the e-beam P_{eb}. This ratio is

$$\frac{P_d}{P_{eb}} = \frac{V_D E}{(\beta - \nu_{i0}) E_i} \tag{B-13}$$

where V_D is the discharge electron drift velocity; E is the applied electric field and E_i is the energy required to create an electron-ion pair by the beam electrons. For discharge stability we have shown that $\beta \geq 2\nu_{i0}$, (19) where β is the electron-attachment rate and ν_{i0} the equilibrium ionization rate, so Eq. (B-13) can be rewritten as

$$\frac{P_d}{P_{eb}} \leq \frac{V_D E}{\nu_{i0} E_i} \tag{B-14}$$

Figures B-2 and B-3 show the predictions of the Boltzmann code for the efficiency of producing metastables, and the ionization rate as a function of the fractional metastable population. With these curves the ionization rate can be expressed as a function of the metastable production efficiency η_M for a given electric field. Thus we can plot the discharge-enhancement ratio as a function of the metastable production efficiency.

Figure B-4 shows such a plot for an electric field of 3 kilovolts per centimeter. Clearly, one can obtain a stable discharge with enhancement greater than five and metastable-production efficiency 70% to 80%. This is obtained at a price; the power into the laser mix decreases as one moves along the curve from left to right. It appears reasonable, however, to obtain such enhancement factors and metastable pumping efficiencies at discharge-power inputs near 100 J/liter-atm-μsec.

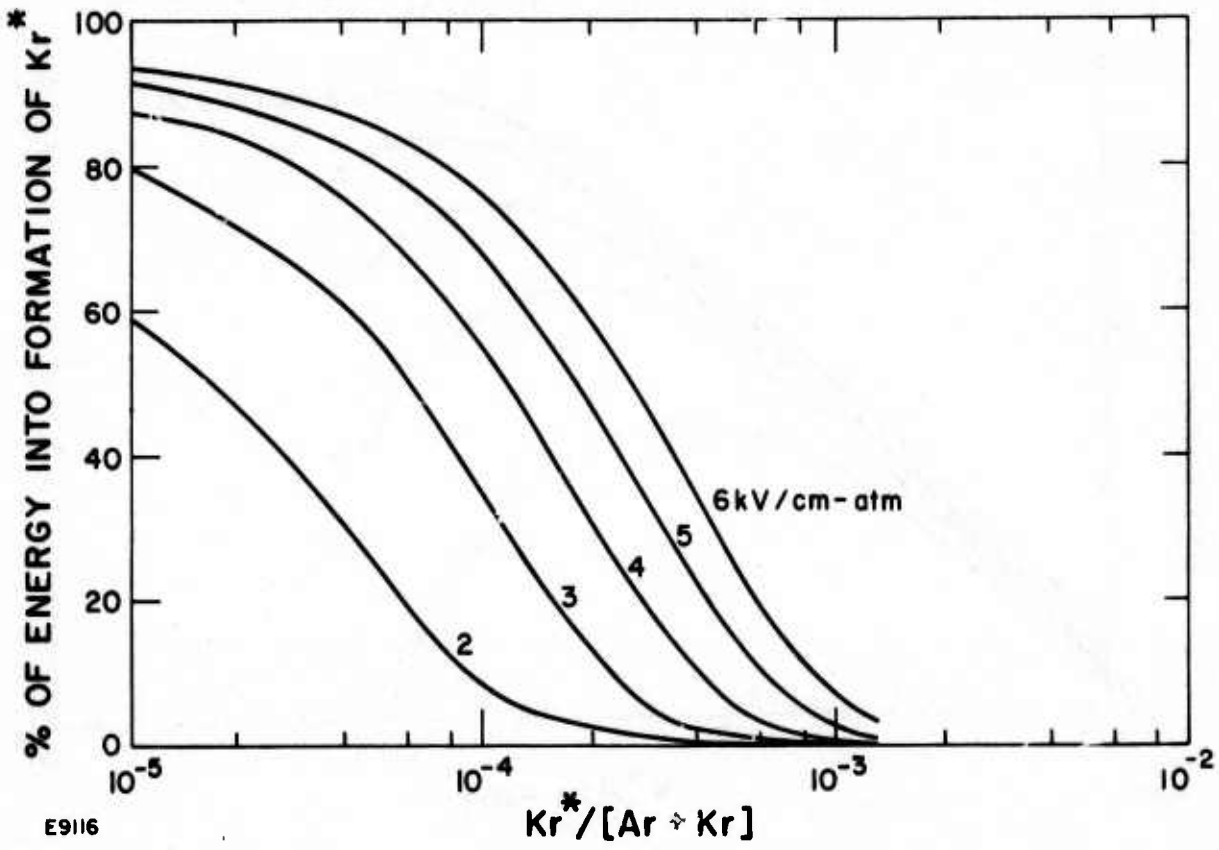

Figure B-2 Percentage of Discharge Power into Kr* as a Function of Fractional Kr* Population for Various Electric Fields

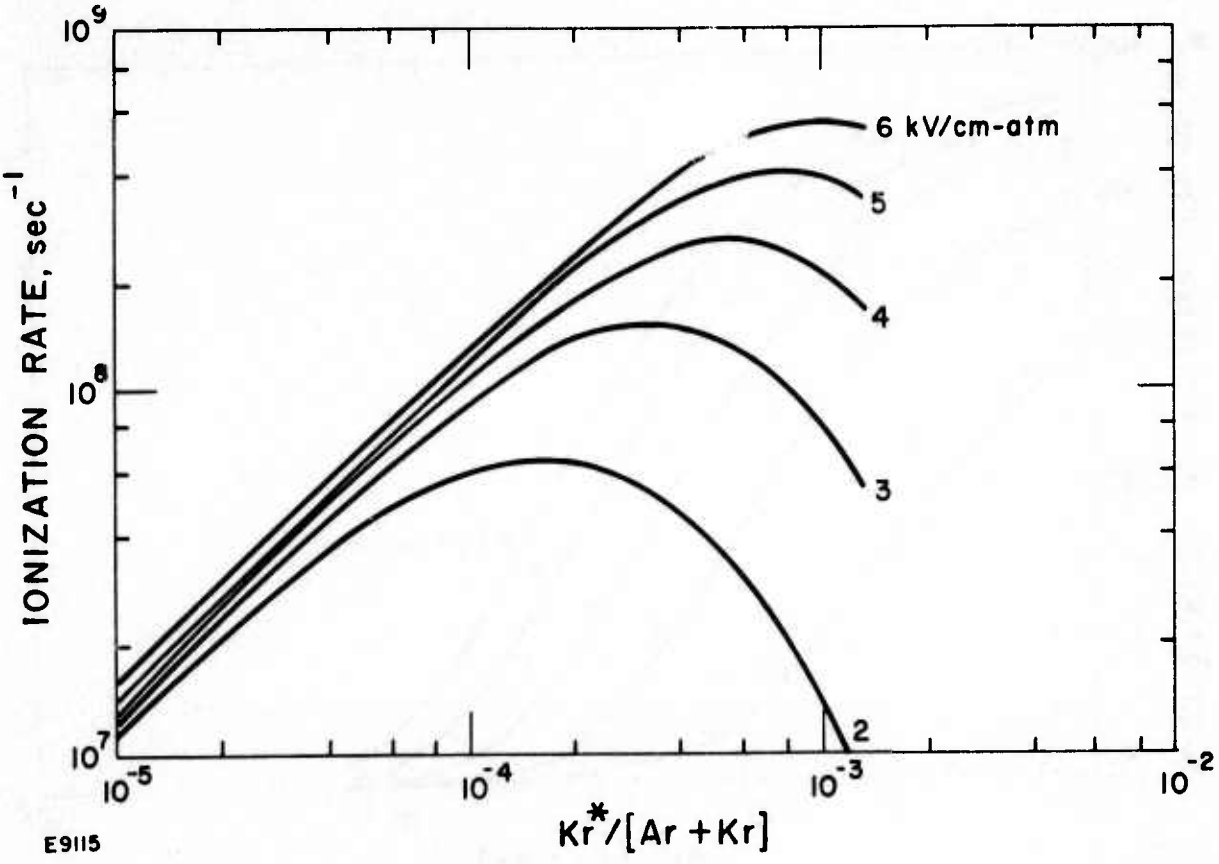

Figure B-3 Ionization Rate as a Function of Fractional Kr* Population

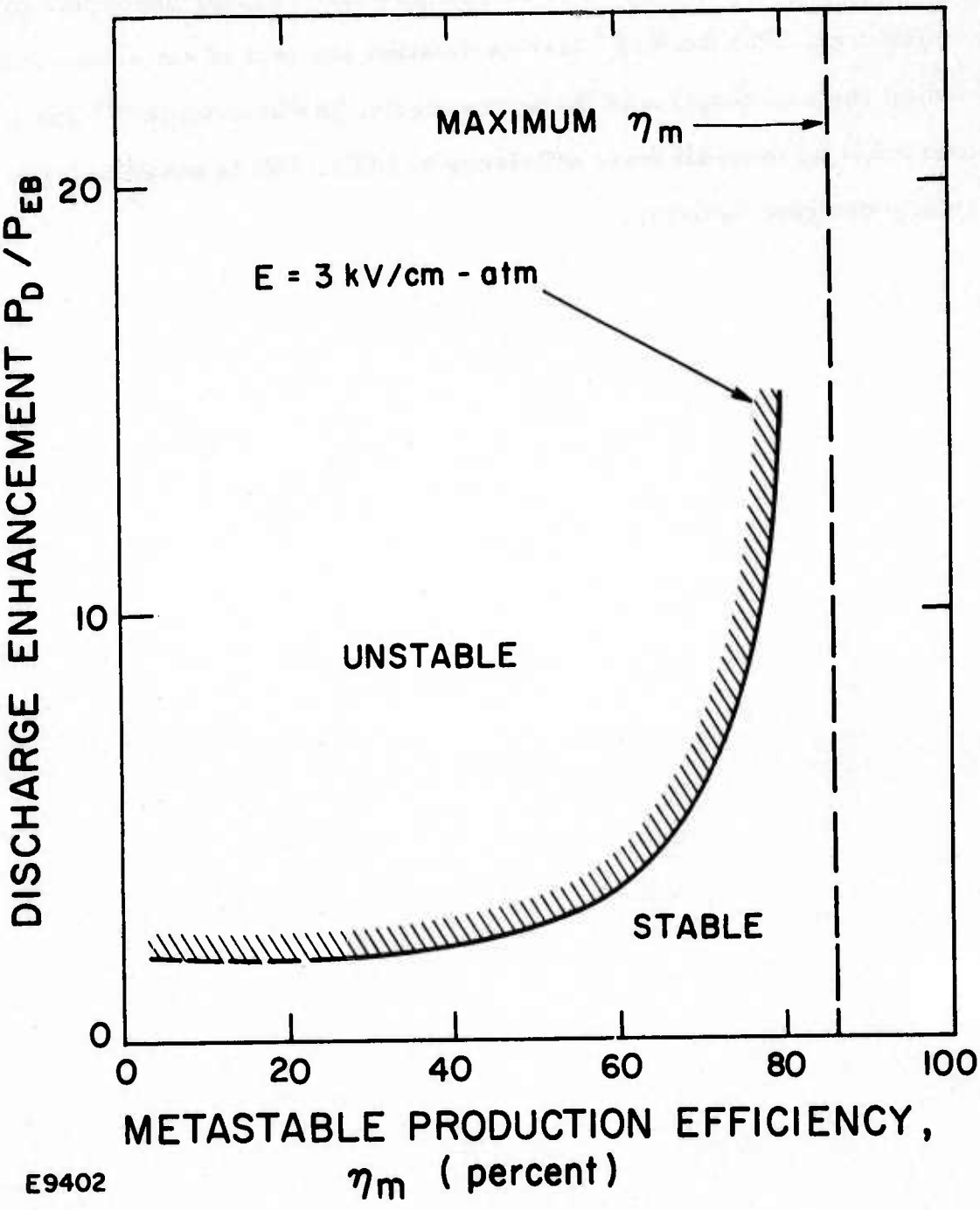

Figure B-4 Discharge Enhancement as a Function of Metastable-Production Efficiency in a Stable Discharge

To compute over-all efficiency, extraction of laser power has to be considered. For the KrF^* laser a detailed analysis of extraction efficiency including photo-absorption of the active media, has been made[23] and it appears that an over-all laser efficiency of 10% to 15% is possible for a carefully designed system.

(23) J.A. Mangano (unpublished)

APPENDIX B

REFERENCES

(1) J.J. Ewing and C.A. Brau, Phys. Rev., A12, 129 (1975).

(2) J.E. Velazco and D.W. Setser, J. Chem. Phys., 62, 1990 (1975).

(3) C.A. Brau and J.J. Ewing, Appl. Phys. Lett. 27, 435 (1975).

(4) J.J. Ewing and C.A. Brau, Appl. Phys. Lett. 27, 350 (1975).

(5) S.K. Searles and G.A. Hart, Appl. Phys. Lett. 27, 243 (1975).

(6) E.R. Ault, R.S. Bradford and M.L. Bhaumik, Appl. Phys. Lett. 27, 413 (1975).

(7) M.V. McCusker et al, Appl. Phys. Lett. 27, 363 (1975).

(8) J.J. Ewing and C.A. Brau, Appl. Phys. Lett. 27, 557 (1975).

(9) J.R. Murray, J.C. Swingle and G.E. Turner, Jr., Appl. Phys. Lett. 28, 530 (1976).

(10) J.M. Hoffman, A.K. Hays, and G.C. Tisone, Appl. Phys. Lett. 28, 538 (1976).

(11) M.L. Bhaumik, R.S. Bradford, Jr. and E.R. Ault, Appl. Phys., Lett 28, 23 (1976).

(12) C.A. Brau and J.J. Ewing (unpublished)

(13) J.A. Mangano and J.H. Jacob, Appl. Phys. Lett. 27, 495 (1975).

(14) J.J. Ewing, H.H. Jacob, J.A. Mangano, and H.A. Brown, Appl. Phys. Lett. 28, 581 (1976).

(15) R. Burnham, D. Harris and N. Djeu, Appl. Phys. Lett 28, 86 (1976).

(16) D.G. Sutton, S.N. Suchard, O.L. Gibb, and C.P. Wang, Appl. Phys. Lett. 28, 522 (1976).

(17) Jim Hsia, Avco-Everett Research Laboratory, private communication.

(18) J.H. Jacob and J.A. Mangano, Appl. Phys. Lett. 28, 724 (1976).

(19) J. D. Daugherty, J. A. Mangano, and J. H. Jacob, Appl. Phys. Lett. 28, 581 (1976).

(20) J. E. Velazco, J. H. Kolts and D. W. Setser (unpublished)

(21) See for example M. Bourene, O. Dutuit and J. LeCalve, J. Chem. Phys., 63, 1668 (1975).

(22) L. A. Gundel et al (unpublished)

(23) J. A. Mangano (unpublished)

DISTRIBUTION LIST

Office of Naval Research, Department of the Navy, Arlington, VA 22217 - Attn: Physics Program (3 copies)

Naval Research Laboratory, Department of the Navy, Washington, D.C. 20375 - Attn: Technical Library (1 copy)

Office of the Director of Defense, Research and Engineering, Information Office Library Branch, The Pentagon, Washington, D.C. 20301 (1 copy)

U.S. Army Research Office, Box CM, Duke Station, Durham, N.C. 27706 (1 copy)

Defense Documentation Center, Cameron Station, Alexandria, VA 22314 (12 copies)

Defender Information Analysis Center, Battelle Memorial Institute, 505 King Avenue, Columbus, OH 43201 (1 copy)

Commanding Officer, Office of Naval Research Branch Office, 536 South Clark Street, Chicago, IL 60615 (1 copy)

New York Area Office, Office of Naval Research, 715 Broadway (5th Floor), New York, NY 10003 - Attn: Dr. Irving Rowe (1 copy)

San Francisco Area Office, Office of Naval Research, 760 Market Street, Room 447, San Francisco, CA 94102 (1 copy)

Air Force Office of Scientific Research, Department of the Air Force, Washington, D.C. 22209 (1 copy)

Office of Naval Research Branch Office, 1030 East Green Street, Pasadena, CA 91106 - Attn: Dr. Robert Behringer (1 copy)

Code 102 IP (ONRL), Office of Naval Research, 800 N. Quincy Street, Arlington, VA 22217 (6 copies)

Defense Advanced Research Projects Agency, 1400 Wilson Blvd., Arlington, VA 22209 - Attn: Strategic Technology Office (1 copy)

Office Director of Defense, Research & Engineering, The Pentagon, Washington, D.C. 20301 - Attn: Assistant Director (Space and Advanced Systems) (1 copy)

Office of the Assistant Secretary of Defense, System Analysis (Strategic Programs), Washington, D.C. 20301 - Attn: Mr. Gerald R. McNichols (1 copy)

U.S. Arms Control and Disarmament Agency, Dept. of State Bldg., Rm. 4931, Washington, D.C. 20451 - Attn: Dr. Charles Henkin (1 copy)

Energy Research Development Agency, Division of Military Applications, Washington, D.C. 20545 (1 copy)

National Aeronautics and Space Administration, Lewis Research Center, Cleveland, OH 44135 - Attn: Dr. John W. Dunning, Jr. (1 copy)
(Aerospace Res. Engineer)

National Aeronautics & Space Administration, Code RR, FOB 10B, 600 Independence Ave., SW, Washington, D.C. 20546 (1 copy)

National Aeronautics and Space Administration, Ames Research Center, Moffett Field, CA 94035 - Attn: Dr. Kenneth W. Billman (1 copy)

Department of the Army, Office of the Chief of RD&A, Washington, D.C. 20310 - Attn: DARD-DD (1 copy)
DAMA-WSM-T (1 copy)

Department of the Army, Office of the Deputy Chief of Staff for Operations & Plans, Washington, D.C. 20310 - Attn: DAMO-RQD - (1 copy)

Ballistic Missile Defense Program Office (BMDPO), The Commonwealth Building, 1300 Wilson Blvd., Arlington, VA 22209 Attn: Mr. Albert J. Bast, Jr. (1 copy)

U.S. Army Missile Command, Research & Development Division, Redstone Arsenal, AL 35809 - Attn: Army High Energy Laser Programs (2 copies)

Commander, Rock Island Arsenal, Rock Island, IL 61201, Attn: SARRI-LR, Mr. J.W. McGarvey (1 copy)

Commanding Officer, U.S. Army Mobility Equipment R&D Center, Ft. Belvoir, VA 22060 - Attn: SMEFB-MW (1 copy)

Commander, U.S. Army Armament Command, Rock Island, IL 61201 - Attn: AMSAR-RDT (1 copy)

Director, Ballistic Missile Defense Advanced Technology Center, P.O. Box 1500, Huntsville AL 35807 - Attn: ATC-O (1 copy)
ACT-T (1 copy)

Commander, U.S. Army Material Command, Alexandria, VA 22304 - Attn: Mr. Paul Chernoff (AMCRD-T) (1 copy)

Commanding General, U.S. Army Munitions Command, Dover, NH 17801 - Attn: Mr. Gilbert F. Chesnov (AMSMU-R) (1 copy)

Director, U.S. Army Ballistics Res. Lab, Aberdeen Proving Ground, MD 21005 - Attn: Dr. Robert Eichenberger (1 copy)

Commandant, U.S. Army, Air Defense School, Ft. Bliss, TX 79916 - Attn: Air Defense Agency (1 copy)
ATSA-CTD-MS (1 copy)

Commanding General, U.S. Army Combat Dev. Command, Ft. Belvoir, VA 22060 - Attn: Director of Material, Missile Div. (1 copy)

Commander, U.S. Army Training & Doctrine Command, Ft. Monroe, VA 23651 - Attn: ATCD-CF (1 copy)

Commander, U.S. Army Frankford Arsenal, Philadelphia, PA 19137 - Attn: Mr. M. Elnick SARFA-FCD Bldg. 201-3 (1 copy)

Commander, U.S. Army Electronics Command, Ft. Monmouth, NJ 07703 - Attn: AMSEL-CT-L, Dr. R.G. Buser (1 copy)

Commander, U.S. Army Combined Arms Combat Developments Activity, Ft. Leavenworth, KS 66027 (1 copy)

National Security Agency, Ft. Geo. G. Meade, MD 20755 - Attn: R.C. Foss A763 (1 copy)

Deputy Commandant for Combat & Training Developments, U.S. Army Ordnance Center and School, Aberdeen Proving Ground, MD 21005
Attn: ATSL-CTD-MS-R (1 copy)

Commanding Officer, USACDC CBR Agency, Ft. McClellan, AL 36201 - Attn: CDCCBR-MR (Mr. F.D. Poer) (1 copy)

DISTRIBUTION LIST (Continued)

Department of the Navy, Office of the Chief of Naval Operations, The Pentagon 5C739, Washington, D.C. 20350 - Attn: (OP 982F3) (1 copy)

Office of Naval Research Branch Office, 495 Summer Street, Boston, MA 02210 - Attn: Dr. Fred Quelle (1 copy)

Department of the Navy, Deputy Chief of Navy Material (Dev.), Washington, D.C. 20360 - Attn: Mr. R. Gaylord (MAT 032B) (1 copy)

Naval Missile Center, Point Mugu, CA 93042 - Attn: Gary Gibbs (Code 5352) (1 copy)

Naval Reaearch Laboratory, Washington, D.C. 20375 - Attn: (Cude 5503-EOTPO) (1 cupy)
Dr. P. Livingston - Code 5560 (1 copy)
Dr. A. I. Schindler - Code 6000 (1 copy)
Dr. H. Shenker - Code 5504 (1 copy)
Mr. D.J. McLaughlin - Code 5560 (1 copy)
Dr. John L. Walsh - Code 5503 (1 copy)

High Energy Laser Project Office, Department of the Navy, Naval Sea Systems Command, Washington, D.C. 20360 - Attn: Capt. A. Skolnick, USN (PM 22) (1 copy)

Superintendent, Naval Postgraduate School, Monterey, CA 93940 - Attn: Library (Coda 2124) (1 copy)

Navy Radiation Technology, Air Force Weapons Lab (NLO), Kirtland AFB, NM 87117 (1 copy)

Naval Surface Wespone Center, White Oak, Silver Spring, MD 20910 - Attn: Dr. Leon H. Schindel (Code 310) (1 copy)
Dr. E. Leroy Harris (Code 313) (1 copy)
Mr. K. Enkenhaus (Code 034) (1 copy)
Mr. J. Wise (Code 047) (1 copy)
Technical Library (1 copy)

U.S. Naval Weapons Center, Chlna Lake, CA 93555 - Atn: Technical Library (1 copy)

HQ USAF (AF/RDPS), The Pentagon, Washington, D.C. 20330 - Attn: Lt. Col. A.J. Chiota (1 copy)

HQ AFSC/XRLW, Andrews AFB, Washington, D.C. 20331 - Attn: Maj. J.M. Walton (1 copy)

HQ AFSC (DLCAW), Andrews AFB, Washington, D.C. 20331 - Attn: Maj. H. Axelrod (1 copy)

Air Force Weapons Laboratory, Kirtland AFB, NM 87117 - Attn: LR (1 copy)
AL (1 copy)

HQ SAMSO (XRTD), P.O. Box 92960, Worldway Postal Center, Los Angeles, CA 90009 - Attn: Lt. Dorlan DeMalo (XRTD) (1 copy)

AF Avlonics Lab (TEO), Wright Patterson AFB, OH 45433 - Attn: Mr. K. Hutchinson (1 copy)

Dept. of the Air Force, Air Force Materials Lab. (AFSC), Wright Patterson AFB, OH 45433 - Attn: Maj. Paul Elder (LPS) (1 copy)
Laser Windo w Group

HQ Aeronautical Systems Div., Wright Patterson AFB, OH 45433 - Attn: XRF - Mr. Clifford Fawcett (1 copy)

Rome Air Development Command, Griffiss AFB, Rome, NY 13440 - Attn: Mr. R. Urtz (OCSE) (1 copy)

HQ Electronics Systems Div. (ESL), L.G. Hanscom Field, Bedford, MA 01730 - Attn: Mr. Alfred E. Anderson (XRT) (1 copy)
Technical Library (1 copy)

Air Force Rocket Propulsion Lab., Edwards AFB, CA 93523 - Attn: B.R. Bornhorst, (LKCG) (1 copy)

Air Force Aero Propulsion Lab., Wright Pattereon AFB, OH 45433 - Attn: Col. Walter Moe (CC) (1 copy)

Dept. of the Air Force, Foreign Technology Divlslon, Wright Patterson AFB, OH 45433 - Attn: PDTN (1 copy)

Commandant of the Marine Corps, Scientific Advisor (Code RD-1), Washington, D.C. 20380 (1 copy)

Aerospace Research Labs., (AP), Wright Patterson AFB, OH 45433 - Attn: Lt. Col. Max Duggins (1 copy)

Defense Intelligence Agency, Washington, D.C. 20301 - Attn: Mr. Seymour Berler (DT1B) (1 copy)

Central Intelligence Agency, Washington, D.C. 20505 - Attn: Mr. Julian C. Nall (1 copy)

Analytic Services, Inc., 5613 Leesburg Pike, Falls Church, VA 22041 - Attn: Dr. John Davis (1 copy)

Aerospace Corp., P.O. Box 92957, Los Angeles, CA 90009 - Attn: Dr. G.P. Millburn (1 copy)

Airesearch Manuf. Co., 9851-9951 Sepulveda Blvd., Los Angeles, CA 90009 - Attn: Mr. A. Colin Stancliffe (1 copy)

Atlantic Research Corp., Shirley Highway at Edsall Road, Alexandria, VA 22314 - Attn: Mr. Robert Naismith (1 copy)

Avco Everett Research Lab., 2385 Revere Beach Parkway, Everett, MA 02149 - Attn: Dr. George Sutton (1 copy)
Dr. Jack Daugherty (1 copy)

Battelle Columbus Laboratories, 505 King Avenue, Columbus, OH 43201 - Attn: Mr. Fred Tietzel (STPIAC) (1 copy)

Bell Aerospace Co., Buffalo, NY 14240 - Attn: Dr. Wayne C. Solomon (1 copy)

Boeing Company, P.O. Box 3999, Seattle, WA 98124 - Attn: Mr. M.I. Gamble (2-, 460, MS 8C-88) (1 copy)

Electro-Optical Systems, 300 N. Halstead, Pasadena, CA 91107 - Attn: Dr. Andrew Jensen (1 copy)

ESL, Inc., 495 Java Drive, Sunnyvale, CA 94086 - Attn: Arthur Einhorn (1 copy)

DISTRIBUTION LiST (Continued)

General Electric Co., Space Division, P.O. Box 8555, Philadelphia, PA 19101 - Attn: Dr. R.R. Sigismonti (1 copy)

General Electric Co., 100 Plastics Avenue, Pittsfield, MA 01201 - Attn: Mr. D.G. Harrington (Rm. 1044) (1 copy)

General Research Corp., P.O. Box 3587, Santa Barbara, CA 93105 - Attn: Dr. R. Holbrook (1 copy)

General Research Corp., 1501 Wilson Blvd., Suite 700, Arlington, VA 22209 - Attn: Dr. Giles F. Crimi (1 copy)

Hercules, Inc., Industrial System Dept., Wilmingtnn, DE 19899 - Attn: Dr. R.S. Voris (1 copy)

Hercules, Inc., P.O. Box 210, Cumberland, MD 21502 - Attn: Dr. Ralph R. Preckel (i copy)

Hughee Research Labs., 3011 Malibu Canyon Road, Malibu, CA 90265 - Attn: Dr. D. Forster (1 copy)

Hughes Aircraft Co., Aerospace Croup - Systems Division, Canoga Park, CA 91304 - Attn: Dr. Jack A. Alcalay (1 copy)

Hughes Aircraft Co., Centineia and Teale Streets, Bldg. 6, MS E-125, Culver City, CA 90230 - Attn: Dr. William Yates (1 copy)

Institute for Defense Analyses, 400 Army-Navy Drive, Arlington, VA 22202 - Attn: Dr. Alvin Schnitzler (1 copy)

Johns Hopkins University, Applied Physics Lab., 8621 Georgia Avenue, Silver Spring, MD 20910 - Attn: Dr. Albert M. Stone (1 copy)

Lawrence Livermore Laboratory, P.O. Box 808, Livermore, CA 94550 - Attn: Dr. R.E. Kidder (1 copy)
Dr. E. Teller (1 copy)
Dr. Joe Fleck (1 copy)

Los Alamoe Scientific Laboratory, P.O. Box 1663, Los Alamos, NM 87544 - Attn: Dr. Keith Boyer (1 copy)

Lulejian and Aseociatee, Inc., Del Amo Financial Center, 21515 Hawthorne Blvd. - Suite 500, Torrance, CA 90503 (1 copy)

Lockheed Palo Alto Res. Lab., 3251 Hanover St., Palo Alto, CA 94303 - Attn: L.R. Lunsford, Orgn. 52-24, Bldg. 201 (1 copy)

Mathematical Sciences Northwest, Inc., P.O. Box 1887, Bellevue, WN 98009 - Attn: Dr. Abraham Hertzberg (1 copy)

Martin Marietta Corp., P.O. Box 179, Mail Station 0471, Denver, CO 80201 - Attn: Mr. Stewart Chapin (1 copy)

Massachusetts Institute of Technoiogy, Lincoln Laboratory, P.O. Box 73, Lexington, MA 02173 - Attn: Dr. S. Edelberg (1 copy)
Dr. L.C. Marquet (1 copy)

McDonnell Douglas Aetronautics Co., 5301 Bolsa Avenue, Huntington Beach, CA 92647 - Attn: Mr. P.L. Klevatt, Dept. A3-830-BBFO, M/S 9 (1 copy)

McDonnell Douglas Research Labs., Dept. 220, Box 516, St. Louis, MO 63166 - Attn: Dr. D.P. Ames (1 copy)

MITRE Corp., P.O. Box 208, Bedford, MA 01730 - Attn: Mr. A.C. Cron (1 copy)

North American Rockwell Corp., Autonetics Div., Anaheim, CA 92803 - Attn: Mr. T.T. Kumagi, C/476 Mail Code HA18 (1 copy)

Northrop Corp., 3401 West Broadway, Hawthorne, CA 90250 - Attn: Dr. Cerard Hasserjian, Laser Systems Dept. (1 copy)

Dr. Anthony N. Pirri, Physical Sciences, Inc., 18 Lakeside Office Park, Wakefield, MA 01880 (1 copy)

RAND Corp., 1700 Main Street, Santa Monica, CA 90406 - Attn: Dr. C.R. Culp/Mr. C.A. Carter (1 copy)

Raytheon Co., 28 Seyon Street, Waltham, MA 02154 - Attn: Dr. F.A. Horrigan (Ree. Div.) (1 copy)

Raytheon Co., Boston Post Road, Sudbury, MA 01776 - Attn: Dr. C. Sonnenschien (Equip. Div.) (1 copy)

Raytheon Co., Bedford Labs, Missile Systems Div., Bedford, MA 01730 - Attn: Dr. H.A. Mehlhorn (1 copy)

Riverside Research Institute, 80 West End Street, New York, NY 10023 - Attn: Dr. L.H. O'Neill (1 copy)
Dr. John Bose (1 copy)
(HPECL Library) (1 copy)

R&D Aseociates, Inc., P.O. Box 3580, Santa Monica, CA 90431 - Attn: Dr. R.E. LeLevier (1 copy)

Rockwell International Corporation, Rocketdyne Division, Albuquerque District Office, 1636 Menaul Blvd., NE, Suite 211, Albuquerque, NM 87110 - Attn: C.K. Kraus, Mgr. (1 copy)

SANDIA Corp., P.O. Box 5800, Albuquerque, NM 87115 - Attn: Dr. Ai Narath (1 copy)

Stanford Research Institute, Menlo Park, CA 94025 - Attn: Dr. F.T. Smith (1 copy)

Science Applications, Inc., 1911 N. Ft. Meyer Drive, Arlington, VA 22209 - Attn: L. Peckam (1 copy)

Science Applications, Inc., P.O. Box 328, Ann Arbor, MI 48103 - Attn: R.E. Meredith (1 copy)

Science Applications, Inc., 6 Preston Court, Bedford, MA 01703 - Attn: R. Greenberg (1 copy)

Science Applications, Inc., P.O. Box 2351, La Jolla, CA 92037 - Attn: Dr. John Aemus (1 copy)

Syetems, Science and Software, P.O. Box 1620, La Jolla, CA 92037 - Attn: Alan F. Klein (1 copy)

Systems Conaultants, Inc., 1050 31st Street, NW, Washington, D.C. 20007 - Attn: Dr. R.B. Keller (1 copy)

Thiokol Chemical Corp., WASATCH Division, P.O. Box 524, Brigham City, UT 84302 - Attn: Mr. J.E. Hansen (1 copy)

TRW Systems Croup, One Space Park, Bldg. R-1, Rm. 1050, Redondo Beach, CA 90278 - Attn: Mr. Norman Campbell (1 copy)

United Technologies Research Center, 400 Main Street, East Hartford, CT 06108 - Attn: Mr. C.H. McLafferty (3 copies)

DISTRIBUTION LIST (Continued)

United Technologies Research Center, Pratt and Whitney Aircraft Div., Florida R&D Center, West Palm Beech, FL 33402 Attn: Dr. R. A. Schmidtke (1 copy)
Mr. Ed Pinsley (1 copy)

VARIAN Associates, EIMAC Division, 301 Industrial Way, San Carlos, CA 94070 - Attn: Mr. Jack Quinn (1 copy)

Vought Systems Division, LTV Aerospace Corp., P. O. Box 5907, Dallas, TX 75222 - Attn: Mr. F. G. Simpson, MS 254142 (1 copy)

Westinghouse Electric Corp., Defense and Space Center, Balt-Wash. International Airport - Box 746, Baltimore, MD 21203 - Attn: Mr. W. F. List (1 copy)

Westinghouse Research Labs., Beulah Road, Churchill Boro, Pittsburgh, PA 15235 - Attn: Dr. E. P. Riedel (1 copy)

United Technologies Research Center, East Hartford, CT 06108 - Attn: A. J. DeMaria (1 copy)

Airborne Instruments Laboratory, Walt Whitorian Road, Melville, NY 11746 - Attn: F. Pace (1 copy)

General Electric R&D Center, Schenectady, NY 12305 - Attn: Dr. Donald White (1 copy)

Clevelend State University, Cleveland, OH 44115 - Attn; Dean Jack Soules (1 copy)

EXXON Research and Engineering Co., P. O. Box 0, Linden, NJ 07036 - Attn: D. Grafstein (1 copy)

University of Meryland, Department of Physics and Astronomy, College Park, MD 20742 - Attn: D. Currie (1 copy)

Sylvenia Electric Products, Inc., 100 Fergeson Drive, Mountain View, CA 94040 - Attn: L. M. Osterink (1 copy)

North American Rockwell Corp., Autonetics Division, 3370 Miraloma Avenue, Anaheim, CA 92803 - Attn: R. Gudmundsen (1 copy)

Massachusetts Institute of Technology, 77 Massachusetts Avenue, Cambridge, MA 02138 - Attn: Prof. A. Javan (1 copy)

Lockheed Missile & Space Co., Palo Alto Research Laboratories, Palo Alto, CA 94304 - Attn: Dr. R. C. Ohlman (1 copy)

ILC Laboratories, Inc., 164 Commercial Street, Sunnyvale, CA 94086 - Attn: L. Noble (1 copy)

University of Texas et Dallas, P. O. Box 30365, Dallas, TX 75230 - Attn: Prof. Carl B. Collins (1 copy)

Polytechnic Institute of New York, Rt. 110, Farmingdale, NY 11735 - Attn: Dr. William T. Welter (1 copy)